2010

An investigation of H2S adsorption mechanisms on Tire Derived Rubber Particles (TDRP^{TM})

Ning Wang
Iowa State University

An investigation of H_2S adsorption mechanisms on Tire Derived Rubber Particles (TDRP^{TM})

by

Ning Wang

A thesis submitted to the graduate faculty

in partial fulfillment of the requirements for the degree of

MASTER OF SCIENCE

Major: Civil Engineering (Environmental Engineering)

Program of Study Committee:

Timothy Ellis, Major Professor
Ning Fang
Shihwu Sung

Iowa State University

Ames, Iowa

2010

TABLE OF CONTENTS

LIST OF TABLES

LIST OF FIGURES

ABSTRACT

Two commercial rubber waste products, tire derived rubber particle (TDRP™) and other rubber material (ORM™), were found to adsorb hydrogen sulfide gas (H_2S) from biogas. A number of experiments were conducted to investigate the adsorption mechanism, surface properties, and breakthrough characteristics. The physical properties, composition, and surface chemistry were investigated and compared with commonly available commercial H_2S adsorbents, such as activated carbon and metal oxide, in order to compare performance and to assess the possible adsorption mechanism. Additional effects on H_2S adsorption capacity of TDRP™ and ORM™ were also studied, including moisture content, zinc concentration, and size distribution.

The components of TDRP™ were similar to typical tire rubber. The specific surface area was less than 1% of activated carbon. The data support the thesis that TDRP™ is particle in nature rather than a porous material. Infrared analysis and Mass spectrum experiments showed no direct evidence that the adsorption was a pure physical process. The effects of moisture content, zinc concentration, and surface oxidation on adsorption favor chemical reactions occurring on the surface of the TDRP™ and ORM™ samples. Analysis of experimental results and comparison to scientific literature, suggest that two components contribute to the H_2S adsorption--carbon black and zinc. The addition and extraction of zinc altered the H_2S adsorption capacity. Oxidation of the surface of TDRP™ and ORM™ also improved the adsorption capacity.

.

CHAPTER 1. OVERVIEW

1.1 Hydrogen sulfide

Hydrogen sulfide (H_2S) is a harmful and malodorous gaseous compound. The colorless and flammable gas is well-known for its odor which resembles a rotten egg smell. A concentration as low as 0.5 ppbv in air can be detected by the human nose. Hydrogen sulfide is soluble in some polar organic solvents and unstable in water. More details of physical properties are shown in Table 1a (Patnaik, 2002).

Hydrogen sulfide can cause human health problems, such as irritated eyes, coma, and respiratory system irritation. It can result in both chronic and acute effects following exposure. For both types of effect, the inhalation minimal risk level is 0.02 ppmv and 0.07 ppmv respectively recommended by the Agency for Toxic Substances and Disease Registry (ATSDR) (ATSDR, 2008). A concentration equal to or greater than 500 to 1,000 ppmv H_2S threatens human life and causes immediate damage to the human body (EPA, 2003). To protect workers, the Occupational Safety & Health Administration (OSHA) regulates the exposure limits for general industry as 20 ppmv during an 8-hour workday. Currently, there is no evidence to support an association between H_2S and cancer.

Hydrogen sulfide often results from decaying organic matter under anaerobic conditions, and it is found in oil, natural gas, and biogas. The biogas, from wastewater treatment plants and landfills, typically contains 0 - 2000 ppmv H_2S,

which varies with the type of feedstock. Besides affecting human health negatively, H_2S increases the distribution system maintenance cost of fuel gas, causes industrial facility corrosion, and oxidizes to SO_2 upon combustion, which is regulated by the EPA to protect air quality. The removal of H_2S from biogas would benefit society, industry, and the environment. Common gaseous H_2S treatment methods include oxidation and sorption.

1.2 Tire Derived Rubber Particles (TDRP™)

1.2.1 Used tires and potential environmental problems

Discarded tires are a potential threat to the environment. Stockpiling or landfilling of used tires occupies large areas of land and leaches hazardous waste materials. Tire incineration is difficult to control and releases hazardous chemicals, such as polycyclic aromatic hydrocarbons (PAH), into the atmosphere (Miguel et al., 2002, Shah et al., 2006). Furthermore, the growth of vehicle and agricultural industries tends to increase the amount of scrap and used tires, which intensifies environmental pressure gradually. Approximated 300 million scrap tires are generated in the US each year. Consequently, proper disposal, reuse, and recycling methods are needed. In 2003, about 80% of the 290 million used tires were recycled or reused in civil construction projects or as tire derived fuel. Of all the reused tires, 30% were ground to rubber particles. The rest of the used tires were retreaded, exported or disposed by landfilling (EPA, 2008). Nevertheless, there are still more than 400 million stockpiled

scrap tires. Reuse and recycle methods include conversion to fuel, incorporation in to civil engineering projects as a construction material, pyrolysis to produce activated carbon, conversion into ground rubber (e.g., for use in asphalt), and application for agricultural and miscellaneous uses.

1.2.2 Tire Derived Rubber Particles (TDRP^{TM})

To develop market alternatives, new applications for reuse of scrap and used tires have been investigated in previous research. Some preliminary research findings have shown that ground tire rubber acts as an adsorbent, for instance, tire rubber was used in soil and water to adsorb metals or organic chemicals (Lisi et al., 2004, Meng et al., 1998). However, little research focused on gas cleaning using ground tire rubber as the scrubber media. Previous work in our research group identified the possibility of hydrogen sulfide removal from biogas by using tire derived rubber particles (TDRP^{TM}) and other rubber material (ORM^{TM}) from Envirotech Inc. (Lawton, Iowa) (Ellis, et al., 2008). Since the raw materials for TDRP^{TM} are waste tires, it has a low initial cost providing it with an economic advantage as an H_2S sorbent, compared to other commercial products. Two types of rubber, ORM^{TM} and TDRP^{TM}, were provided by Envirotech for use in the research. ORM^{TM} is a type of original rubber material from an industrial manufacturing process. The production process is a trademark secret and production details are not provided.

1.3 H_2S removal by TDRP™

TDRP™ was used as an adsorbent and expected to replace the application of activated carbon or metal adsorbents in scrubber systems. It has significant environmental and economic benefits because of the low price. After H_2S removal, the spent TDRP™ could be used to produce asphalt or work as the construction material in other applications. A batch adsorption investigation was conducted by the same research group. For 1400~5000 ppmv H_2S, the removal efficiency exceeded 99%. It was determined that the adsorption process was modeled using a Freundlich adsorption isotherm (Ellis et al., 2008) .

1.4 Objectives

The overall objective was to investigate the adsorption mechanism of hydrogen sulfide on rubber particles using laboratory experiments. Since there was no similar previous study, this work followed the general theory for sorbent and adsorption material behavior. More specifically, the objectives of this study were:

- To characterize the chemical, physical, and surface properties of TDRP™ and compare the material with other commercial H_2S adsorbents.
- To investigate the effects of different factors on H_2S adsorption using TDRP™ including size distribution, moisture content, and zinc concentration.

- To analyze the adsorption behavior of H_2S relating to the properties of TDRP^{TM} and investigate the mechanism of adsorption.

The purpose of this research was not only to give a systematic understanding of the new H_2S sorbent, but to investigate the factors that could improve the removal efficiency of H_2S. An understanding of the adsorption mechanism was important in this pursuit. Although the research focused on the commercially available used rubber particle samples, the results could provide useful for research on other rubber particle materials.

CHAPTER 2. LITERATURE REVIEW

2.1 Adsorption

Adsorption is one of the separation methods for contaminant removal. The process is described as the adhesion of atoms, molecules or ions of gas, liquid or solid on a surface material (Brandt et al., 1993). The adsorption process is generally classified as physical adsorption (physisorption) or chemical adsorption (chemisorption) by adsorbate-adsorbent interaction types -- Van der Waals forces or chemical (ionic or covalent) bonding. However, these two processes coexist in practical adsorption applications and are difficult to distinguish.

2.1.1 Adsorption and absorption

The word “sorption” includes adsorption and absorption, and both belong to the category of diffusion-equilibration processes (Tien, 1994). It is hard to differentiate these two terms either by laypersons or researchers. In contrast to adsorption, absorption is a bulk separation method, which means an atom, molecule, or ion will enter into some bulk phase (gas, liquid or solid) materials. Different industrial operations are required for the two different processes in practical applications. Some differences between the two terms in engineering applications are shown in Table 1.

Table 1. Differences between adsorption and absorption.

	Adsorption	Absorption
Extent determination methods	Isotherm relationship	Solubility
Adsorbent packing	Stationary	Moving
Sorption area	Surface	Volume
Allied reverse operation	Regenerations of adsorbent	Stripping, desorption, etc.
Packing media	No	Normally with solid packing to increase the absorption efficiency
Operation control	Non-steady-state	Steady state

2.1.2 Equilibrium isotherms and diffusion

Generally, there are three mechanisms in the adsorptive separation: steric, kinetic, and equilibrium effect (Yang, 2003). All the processes may combine and contribute to one adsorptive separation operation. The comparison among the three processes is shown in Table 2. Since there is no clear boundary between each of the three mechanisms, in a specific adsorption situation, the equilibrium isotherm, and pollutant diffusivity are typically considered for sorbent selection and investigation.

Table 2. Difference among three adsorption mechanisms.

	Steric separation	Kinetic separation	Equilibrium separation
Applications	Drying with 3A zeolite The separation of normal paraffins by 5A zeolite	Air separation by pressure-swing adsorption with zeolite	Widely used for the targeted molecular with polarizability, magnetic susceptibility, permanent dipole moment or quadruple moment
Classic adsorbents	Zeolites and molecular sieves	Zeolite/carbon molecular sieve	Activated carbon/zeolite/
Separation mechanism	By different molecular sizes	By different diffusion rates	By the equilibrium adsorption of mixture
	This type of separation is generally treated as equilibrium separation	Considered when equilibrium separation is not feasible	Sorbent selection depending on the fundamental properties of the targeted molecule

2.2 Surface characteristics and analysis methods

2.2.1 Langmuir isotherm

The Langmuir isotherm is widely used to investigate the adsorption behavior of molecules on a solid surface at a fixed temperature. It was derived by Irving Langmuir in 1916 (Wikipedia, 2010). The equation is stated as follows,

$$\theta = \frac{\alpha P}{1+\alpha P} \qquad \text{Equation 1}$$

Where, θ= the fractional coverage of the surface

P= the gas pressure or concentration

α= the Langmuir adsorption constant

2.2.2 BET theory

BET theory was published by Brunauer et al. (1938) and is the basis of the measurement of a solid material's specific surface area. It is the rule for physical multilayer to adsorb gas molecules on a solid surface. Based on Langmuir's Theory, they derived the equation:

$$\frac{p}{v(p_0-p)} = \frac{1}{v_m c} + \frac{c-1}{v_m c}\frac{p}{p_0} \qquad \text{Equation 2}$$

Here, p and p_0 are the equilibrium and the saturation pressure of adsorbates, v is the adsorbed gas volume and v_m is the monolayer adsorbed gas volume. The variable, c, is the BET constant.

Because p_0 and c are known values at a certain temperature, v_m can be calculated from a linear plot of p and v. Consequently, the BET specific surface area would be investigated by the following equation:

$$S_{BET} = \frac{v_m N s}{aV} \qquad \text{Equation 3}$$

Here, N is Avogadro's number; V is molar volume of adsorbent gas and a is the molar weight of the adsorbed species; and s is the adsorption cross section of the adsorbed molecules, which could be calculated from the density of the solidified gas and of the liquefied gas.

A larger surface area provides more contact opportunities between sorbents and sorbates. It results in higher sorption capacity for many sorbents. Nitrogen adsorption is a powerful method to analyze the specific area and pore structure of particles based on the BET theory. It has been applied widely on activated carbon, carbon black, and other porous materials. This method was also used for crumb rubber (Xiao et al., 2009). These investigators reported that the specific surface area of the mesh size (75~1180 μm) of tire particles were 0.0016~0.170 m^2/g.

2.2.3 Oxygen containing functionalities

Oxygen containing functionalities include functional groups containing carbon-oxygen bonds and are responsible for some characteristic chemical reactions. Among these groups, carboxyl, anhydride, lactone, and phenol groups typically contribute to the acidity of the surface, whereas the carbonyl and quinone groups contribute to the basicity (Almarri et al., 2009). The acid functionalities are associated to the adsorption capacity of activated carbon or carbon black by chemical reactions or catalysis effects.

Boehm titration is the most common method to detect the distribution of some important functionalities (Boehm, 1966) of particle and porous materials. According to

the different acidity of functionalities, Boehm used various bases, such as sodium hydroxide, sodium carbonate, and sodium bicarbonate to neutralize them. Then, the concentrations of functionalities on the solid surface can be calculated with the consumption of base titrant. This method has been utilized on carbon, silica, alumina, and titanic dioxide. It can quantify the amount of carboxylic, lactonic, and phenolic groups. Infrared spectroscopy is an instrumental analysis method, which can also be used to detect the surface oxygen groups. Different molecular bonds have a characteristic frequency of vibration or rotation. The specific frequency is associated with a certain wavelength of inlet infrared absorption. Consequently, the technology can identify compounds and molecular structure by detecting the characteristic adsorption (Biniak et al., 1997). Fourier Transform Infrared (FTIR) spectroscopy is used to identify the existence of carbonyls and alcohols (or ethers) on activated carbon surface. There are also some other functionalities analysis methods including X-ray photoelectron spectroscopy (XPS), scanning electron microscope (SEM), and scanning tunneling microscope (STM).

2.2.4 Metal concentration

It was reported that tire rubber contains many types of metal elements. The distribution of the metals and their compounds is not homogeneous. Although there is no research on the role they are playing in the H_2S adsorption behavior, it is true that some metals or metal oxides can adsorb gas on the surface.

Metals can distribute on the surface or inside the tire rubber. The total concentration of metal in rubber could be detected by atomic adsorption spectroscopy (AAS) or inductively coupled plasma atomic emission spectroscopy (ICP-AES). Under a certain condition, the metal atom could adsorb or emit photons with a characteristic wavelength, and this can change the spectroscopy of inlet and outlet light. Both methods make use of the change of spectroscopy of a certain atom relating to the change of the metal element amount. The two methods can be used to determine the amount of trace metal when compared to a standard curve. However, the forms of metal samples will be destroyed during the preparation, like digestion, because the samples are required in solution or liquid phase. Atomic absorption spectroscopy and atomic emission spectroscopy results, therefore, give the total concentration of metal elements.

Since, the adsorption of gas occurs on the surface of adsorbent, it is more important to characterize the distribution of metal elements on the surface. XPS is a surface analyzing technique used for chemical identification of surface species. By recording the X-ray activated electrons emission from chemicals, XPS could be utilized to analyze the elemental composition, empirical formula, chemical state, and electronic state. There are also some other methods that are useful for evaluating surface elements including auger electron spectroscopy (AES), X-ray diffraction (XRD), and scanning electron microscope (SEM).

2.2.5 Acid-base properties

Acid-base properties are normally attributed to the surface functionalities on homogenous material, such as activated carbon and carbon black. For more complex materials, like ground tire rubber, they depend on specific ingredients besides functionalities. Surface pH value is an index to evaluate acidity and basicity. Normally, the pH value of rinse water is considered as the value of solid material.

2.2.6 Summary

The surface characteristic methods and techniques are relatively mature for the analysis of homogenous materials with simple ingredients. However, research on complex multi-component materials is limited. Using only one technique cannot give sufficient or correct information. The combination of many analysis methods is needed to fulfill the task.

2.3 Tire rubber compositions and properties

As a commercial product, vehicle tires are a complex mixture which contains innumerous components and their quantities vary with types. The typical composition of a tire is shown in Table 3.

Table 3. The typical types of materials used to manufacture tires (Rubber Manufacturers Association).

Synthetic Rubber	
Natural Rubber	
Sulfur and sulfur compounds	
Silica	
Phenolic resin	
Oil	aromatic, naphthenic, paraffinic
Fabric	Polyester, Nylon, Etc.
Petroleum waxes	
Pigments	zinc oxide, titanium dioxide, etc.
Carbon black	
Fatty acids	
Inert materials	
Steel Wire	

It was shown that the weight percentage of some main components of tire rubber in the following Table 4 (Lehmann et al., 1998):

Table 4. Composition of Vehicle Tire Rubber (Lehmann et al., 1998).

Component	*wt % (as received)*
styrene-butadiene rubber (SBR)	62.1
carbon black	31.0
extender oils	1.9
zinc oxide	1.9
stearic acid	1.2
sulfur	1.1
other additives	0.7

2.3.1 Polymer

Normally, tires contain a certain amount of natural rubber and synthetic rubber. Natural rubber only contains polyisoprene, while common synthetic rubber compounds originate from two alkenes: butadiene and styrene.

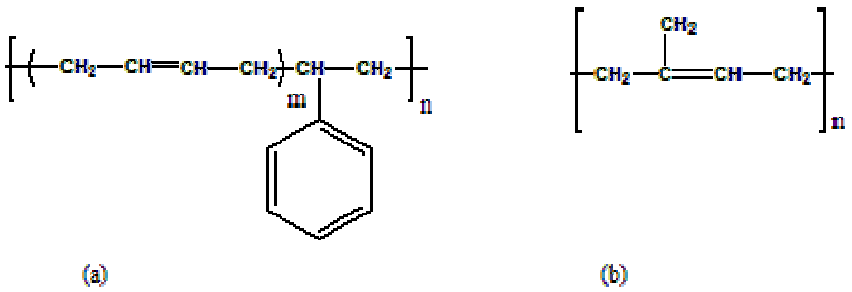

(a) (b)

Figure 1. Chemical structure of polystyrene-butadiene (a) and polysisoprene (b).

After vulcanization, the double bonds in the polymers are broken down and replaced by -S- bonds. Since no active sites exist on the surface of the polymer, there is little opportunity for gas to be adsorbed on the surface of rubber polymer. However, the adsorption is possible if the double bonds are replaced by some active substrates or functional groups.

There are more than twenty kinds of commercial synthetic rubbers. To identify the type of polymer, many methods were used in the past century. Infrared spectroscopy (IR) is a reliable instrumental analysis method. By comparing with the IR-spectrum of standard samples, the polymer sample could be distinguished. The IR method is the favorable alternative when other tests, like Dripping, Flotation, and Halogen test, fail to

work (Verleye et al., 2001). Other widely used instrumental analysis methods are gas chromatograph (GC) and nuclear magnetic resonance spectroscopy (NMR).

2.3.2 Carbon black and surface chemistry

Carbon black is generated from incomplete combustion of organic compounds. Typically, a tire contains 30~35% carbon black and this varies by types (Rodgers, 2004). Carbon black is defined as a "*material consisting of elemental carbon in the form of near-spherical particles coalesced into aggregates of colloidal size, investigated by incomplete combustion or thermal decomposition of hydrocarbons*". It has become a common additive of a tire since last century, because it can significantly increase the reinforcement and other physical properties (Rodgers, 2004). During the manufacture of tire rubber, carbon black is added with shear forces by mixing. Polymer can fill in the voids between the carbon black aggregates and the mixture generates a coherent rubbery composite. Sometimes, the activated sites of black carbon can grow polymers directly by the free radical method. This process is called polymer grafting, which benefits the structural properties.

Compared with activated carbon, the surface of carbon black is much smoother. The specific surface area could be estimated by the measurements of iodine number or nitrogen adsorption. Carbon blacks could be categorized as ten grades by nitrogen surface area, assigned the numbers 0~9 shown in Table 2a.

The oxygen consists 0.2~0.5% wt of carbon black. It is reported that some oxygen functional groups distribute on the surface of carbon black, such as C-H, -CHO, --OH, -COOH, and -C(=O)-. Also, it is reported that 18% of the surface oxygen may be present in -C(=O)- groups and basing on different carbon blacks, an additional 4~19% existed in carboxyl groups, in which phenolic groups dominated (Studebaker et al., 1956). This matches the statement of Papirer's work that the smooth surface of carbon black is comprised with polycondensed aromatic layers (Papirer et al., 1996). The polar chemical surface groups on carbon black, to some extent, grant the adsorption capacity. The molecules H_2, NH_3, and H_2S were reported to interact with carbon black (Rodgers, 2004). To increase the adsorption ability and the number of functional groups, surface oxidation of carbon black is recommended. Although oxidation of nitric acid would decrease specific surface area and pore volume, it dramatically improves the surface oxygen content, which means more functional groups were added (Krishnankutty and Vannice, 1995).

The amount and type of carbon black could be estimated by thermogravimetric analysis (TGA), which is a test to determine the change in weight of samples in relation to the change of temperature. For rubber samples, first of all, oil and polymer are removed by pyrolysis in nitrogen. After a sample is cooled down to 275 ˚C, air is introduced and the tire sample is reheated to 900 ˚C (Loadman, 1998). The procedure is shown in the following figure 2.

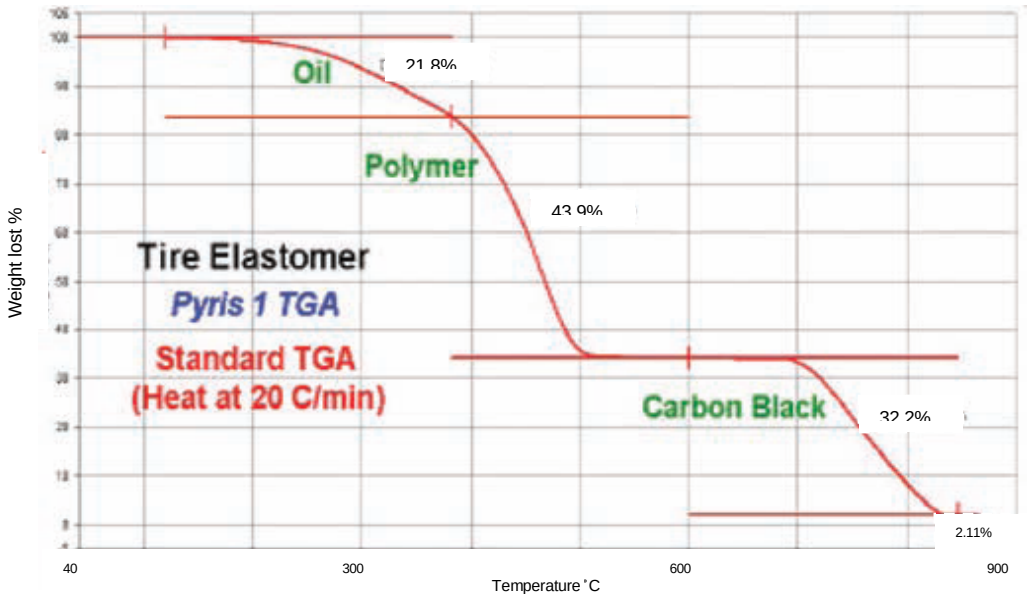

Figure 2. Standard TGA results obtained on tire elastomer by heating at a constant rate of 20 °C/min (Loadman, 1998).

2.3.3 Zinc

Zinc oxide is the most important inorganic activator during vulcanization process of tire manufacture. It was reported that the average value of zinc in car tire tread was 1.2% and in truck tire tread was 2.1% (Smolders and Degryse, 2002). Zinc oxide enhances the efficiency and properties of vulcanization and reduces the time used. The mechanism might follow the simple reactions shown below (Barton, 1950):

$$\text{RH (Rubber hydrocarbon)} + S_x \xrightarrow{Accelerator} \text{RSH} + S_{x-1}$$

$$2\text{RSH} + Zn^{2+} \rightarrow \text{RSZnSR} + 2H^{+}$$

$RSZnSR + S_x \rightarrow RSSR + ZnS + S_{x-1,}$

With the help of the zinc ion, two rubber polymer fibers are connect by sulfur and ZnS is released. Besides ZnS and ZnO, another common form of element zinc in tire rubber is zinc stearate, an octadecanoic acid zinc salt, which takes approximately 2% in weight of tire polymer and is shown in Figure 3:

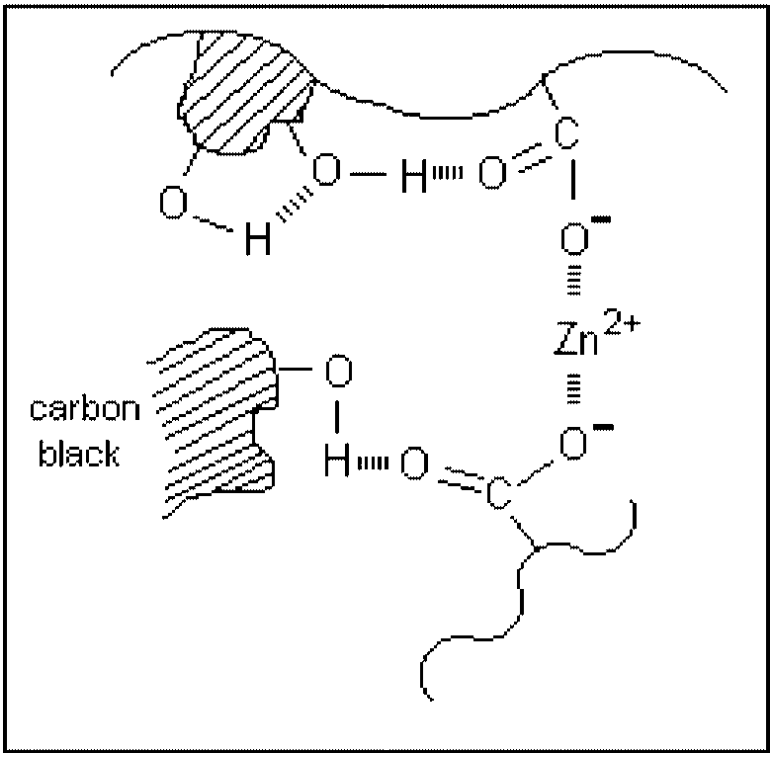

Figure 3. Schematic representation of the interaction between zinc stearate and tire rubber (Segre et al., 2002).

Zinc stearate generation might result from the solubilization of ZnO in fatty acids during vulcanization process. Because solubilized ZnO performs better than ZnO particles, to gain better dispersion and solubility of zinc ions, zinc stearate might

replace ZnO as activator (Rodgers, 2004). Because of the change of crystal structure of zinc oxides and the fact that zinc could react with other compounds, the role of ZnO particles is complex and the forms of Zn element in the tire are various. Nowadays, considering the negative environmental effect of zinc, zinc-free tire rubber or low-zinc tire rubber is becoming a popular research topic. Improvement of vulcanization technology and new activators are attracting more researchers (Barton, 1950, Heideman et al., 2005).

Some methods could be used to detect the amount of element zinc in rubber, such as, EDTA titration, AAS, and plasma spectroscopy, combined with proper rubber digestion methods.

2.3.4 Other elements

Sulfur and silicon are also common elements in tire rubber. Since the 1980s, silica has been considered as a reinforcing filler of tire tread (Leblanc, 2002). It increases rolling resistance by forming siloxane and more and more researchers are focusing on researches of this material. The quantity of silicon in tire rubber can be detected gravimetrically or colorimetrically (Loadman, 1998), because the silicon compound can be converted to silica by heating and acid digestion without volatility. However, the silica amount in used tires could be lower because of the tread abrasion on the road while vehicles are running.

Sulfur plays an important role during the vulcanization of rubber as mentioned above and it could be determined by ultimate analysis.

Other minor elements, such as Hydrogen, Oxygen, and Nitrogen, could also be determinate by proximate and ultimate analysis (Ucar et al., 2005).

Table 5. Proximate and ultimate analyses of scrap tires.

Type of scrap tire	Passenger car tire	Truck tire
Proximate analysis (as received, wt%)		
Moisture	1.6	1.4
Volatile matter	58.2	66.1
Fixed carbon	21.3	27.5
Ash	18.9	5.0
Ultimate analysis (dry, %)		
C	74.3	83.2
H	7.2	7.7
N	0.9	1.5
O	15.9	6.2
S	1.7	1.4

2.3.5 Summary

Current instrument analysis technology can successfully provide useful information on qualification and quantification of tire ingredients. Although there is research referring to the surface properties of component of rubber, the effect of changing these properties is not understood, especially the effects on adsorption behavior.

2.4 Tire reuse

The rubber polymers are thermosetting materials rather than thermoplastic materials, which means it is hard to reheat and mold to a certain shape (Adhikari et al., 2000). This is due to a cross-link process connecting single polymer chains together by chemical bonds. For rubber, they are usually sulfur and carbon bonds. The three dimensional network of thermoset polymers increases the strength and resistance to high temperatures. However, it also brings challenges for the treatment of the waste tire.

2.4.1 Reuse of waste tire rubber

Used tires are required to be shredded by cutting, milling or so on; this is not only for reusing or reclaiming purpose, but also to save space for land filling. In Iowa, since 1991, whole waste tires have been banned from landfills by House Rule 753, (1989). By size, the shredded scrap tires could be classified as, shredded tires (300 to 460 mm long, 100 to 230 mm wide), chipped tires (13 mm to 76 mm), ground rubber (<19 mm) and crumb rubber (<4.75mm) (Siddique and Naik, 2004). Since there is no universal regulation to define this treated tire rubber, the categories above are just a reference. Rubber can be made into rubber chips or particles with mechanical or chemical methods. The freeze and crush method is a new technology in which, liquid nitrogen converts elastic rubber into ice-like material under low temperature. Consequently, tire rubber is crushed as uniform particles.

A low cost and proper shred method could efficiently benefit the application of the rubber and attract more investment to treat the problem of used tire. The following scheme in Figure 4 is a typical process at a scrap tire factory.

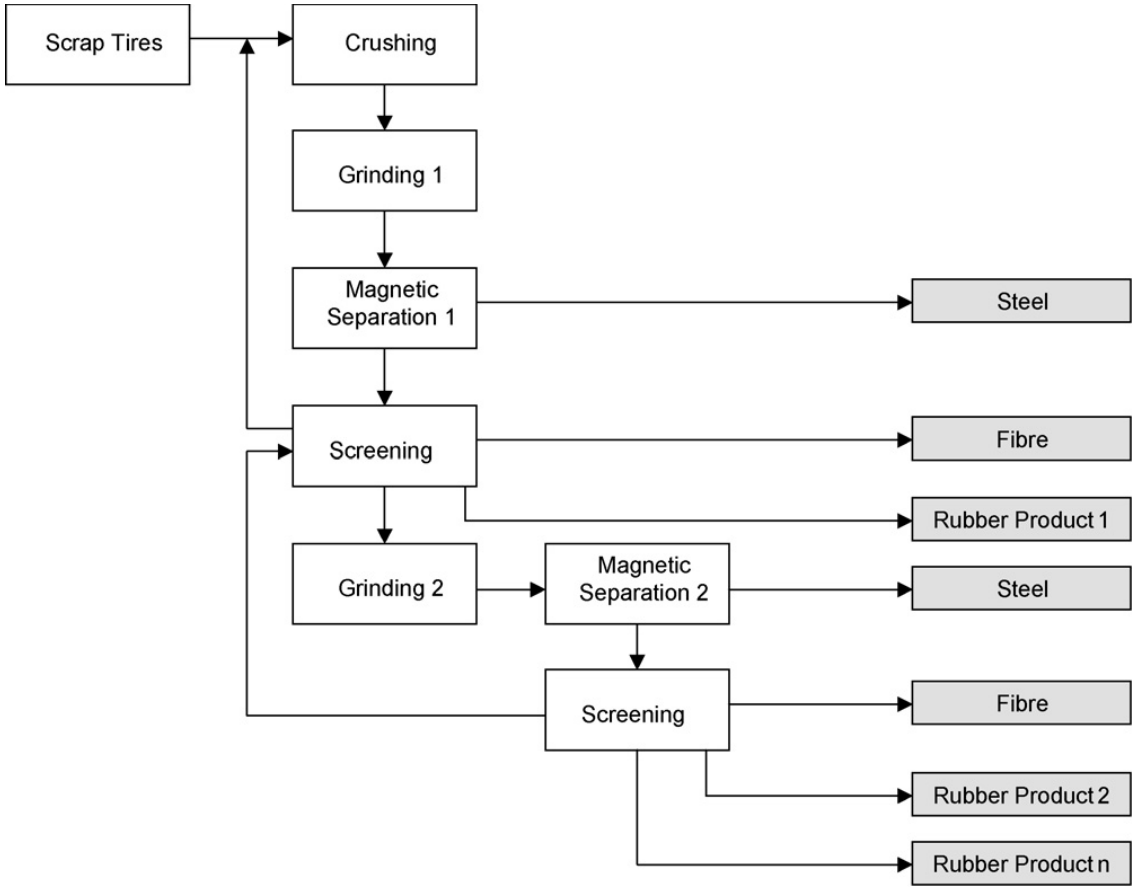

Figure 4. Example of a scrap tire processing plant (Pehlken and Müller, 2009).

Among the reuse or reclaiming methods, use as fuel is another common way of beneficially dealing with waste tires. The high carbon element concentration makes waste tire rubber a potential new energy source. Under pyrolysis conditions (high temperature without oxygen), oils are derived from tire rubber (Ucar et al., 2005). The oils could be used as fuel, petroleum refinery feed stocks, or chemical refinery source.

The solid residue is also a good fuel candidate as char. Waste tire gasification is another consideration of researchers. Flammable gases (CO, CO_2, and hydrocarbon gases) could be produced by pyrolysis. Pyrolyzed gases and derived products are generated at temperature between 500 and 1000 ˚C (Leung et al., 2002). High temperatures and long resident times increase the productivity of gases. However, the optimized heat value was found to be at 700~800 ℃, because a higher yield could result from the lower heat value gas at a high temperature. Tar and char are byproducts generated during the process, and these byproducts make up more than 50 wt % of the products. For commercial applications, it is desirable to produce a pure gas during fuel production. However, the processes could produce undesired byproducts, such as H_2S and CO_2. They reduce the heat value of the gas fuel or result in negative effects on atmosphere. Separation and removal technology and utilities need to be introduced in the tire-based fuel production. The cost and potential environmental problem should also be considered. During the fuel making process, catalyst optimization is an important research field. It is reported that lubricant based oil combined with ZSM-5 zeolite can remarkably increase the pyrolysis rate and the yield of oil products (Leung et al., 2002). Zeolite can help break the carbon bonds of tire rubber and prevent coke formation due to the pore structure.

Civil engineering material applications are an important reuse option for waste tire rubber. Tire rubber-additive concrete is widely used in building construction. In one reuse application, asphalt is mixed with ground tires. Researchers investigated the possibility of using waste tire in stone matrix asphalt (Putman and Amirkhanian, 2004).

They did not find a significant difference between this and hot mix asphalt produced by cellulose and polyester fibers. Besides, rubber fiber improved the strength of the mixtures. In another study, researchers tested the properties of 35% NaOH-treated tire rubber-containing sand-cement mortar (Segre et al., 2004), because this can reduce the water adsorption and sorptivity coefficients, which results in an increase in the resistance to acid attack and protects from freeze and thawing cycles. The negative effect is that flexural strength is also decreased by the amount of rubber in mortar. However, some researcher argued that the tensile and flexural strengths of the tire rubber ash mortar are higher (Siddique and Naik, 2004). Two kinds of rubber modified concrete were compared (Li et al., 2004). One was added with tire rubber particles or chips and the other contained rubber in the form of fiber. They found fiber worked better than particles or chips. Flowable fill is another choice of tire reuse in civil construction. Researchers stated that crumb rubber was an ideal aggregate for flowable fill because of the reduction in end-product density and strength (Pierce and Blackwell, 2003).

Utilizing used tires as pollutant control material is a brilliant idea. Due to the high concentration of carbon element, tire rubber is a good potential activated carbon raw material. There are many studies focused on the pyrolysis of tire rubber to produce activated carbon. Tire-derived activated carbons are primarily mesoporous and have lower adsorption capacity compared to the coal-derived activated carbons (Lehmann et al., 1998) . However, the former contains about 50% less sulfur than coal material, which causes less pollution to the atmospheric environment.

2.4.2 Tire rubber for adsorption applications

Although it may increase the pollutant removal efficiency, the use of thermal treatment to created activated carbon from tire rubber requires facilities and operation investment. An alternative idea is employing the raw rubber material directly to deal with pollutant. Researchers proved that the rubber particles could be used as adsorbent for metal and organic compounds, and this approach is explored in detail.

Ground tire rubber's ability of sorbing heavy metals was found in the late last century. The immobilization of Mercury (II) was investigated in contaminated soil with ground tire rubber (Meng et al., 1998). Mercury-spiked clay-foam was mixed with a certain amount of rubber. The results showed ground tire rubber could stop short-term Hg leaching under acid and neutral condition. The adsorption of Hg on tire rubber followed the Langmuir isotherm:

$$\Gamma = \Gamma max \frac{K_{ads}[Hg]}{1+K_{ads}[Hg]} \qquad \text{Equation 4}$$

Where $\boldsymbol{\Gamma}$ is the amount of sorbate on sorbent, $\boldsymbol{\Gamma}_{max}$ is the maximum monolayer adsorption capacity and K_{ads} is the adsorption equilibrium constant. In the test, $\boldsymbol{\Gamma}_{max}$ and K_{ads} are 14.6 mg Hg/g and 4.7 l/rag, respectively. They hypothesized the sorption of Hg resulting from sulfur on rubber. However, there is no direct evidence in their research. Recent research focuses on the improvement of sorption capacity. In ultrasound treatment of tire rubber, the removal efficiency of aqueous Cr (III) was improved (Entezari et al., 2005). Ultrasound could increase the number and length of

cracks and fissures on the rubber particle surface and change the morphology. This change resulted in a larger surface area. Ultrasound treatment also favors mass transfer near the particle surface by decreasing the boundary layer. They also reported the porous diffusion step is the limited process of sorption. The sorption concentration (*C*) has a linear relationship with the square root of time ($\sqrt{t}$). It could be explained by the Weber and Morris model el ($C = C_0 - k_w\sqrt{t}$).

Volatile organic compounds (VOCs) have been found in leachates from municipal solid waste and landfills. Large-scale tank tests and field tests (Park, 2004) showed tire chips sorb significant amounts of VOCs, such as BETX compounds (benzene, toluene, ethyl benzene, and m-, p-,o-xylenes), without changing the drainage layer structure properties. Although ground tires could provide more sorption capacity, it cost more and changes the hydraulic conductivity. Tire chips are more suitable as a leachate collection layer in landfill construction. The sorption of organic compounds are significantly affected by pH and temperature (Kim et al., 1997). They also stated that linear model of partitioning is suitable to explain the organic compound sorption on ground tires.

Linear isotherm model: $C_s = K_p C_t$ Equation 5

Where, at equilibrium state, C_s is the sorbate concentration on sorbent; C_t is the sorbate concentration in solution; K_p is the partition coefficient. Besides VOCs, o-xylene and benzene could be sorbed as well according to the study of (Lisi et al., 2004). They calculated that ground rubber has 2.8~5.7% of granular activated

carbon's sorption capacity. Langmuir isotherm fits benzene sorption well while a linear isotherm fits O-xylene better. Considering the price advantage, the ground tire rubber should occupy parts of the sorbent market.

Surfactants are common pollutants in municipal sewage, which cause smell, eutrophication, and health risk. It was found rubber granules could sorb anionic surfactants--sodium dodecyl sulfate (Purakayastha et al., 2005, 2002). They tested the sorption kinetics and found that it follows Langmuir isotherm model and film diffusion is the rate-limiting factor.

Granulated tires are put as a sub-surface drainage layer as beneath sand-based root zones and found nitrate was reduced by 58.6% in leachate samples compared to the no-rubber layer (Lisi et al., 2004). However, the mechanism of nitrate mitigation remains unclear. It was proved that the utilization of granulated tires had no negative effect on the turf grass quality of golf courses. Although the rubber drainage layer cannot solve the nutrient leakage problem, it benefits the solid waste management of waste tires because of the large demand for golf course construction.

Oil spills are a serious ecosystem catastrophe. The pollutants include crude oil, petroleum products, and some by-products. It normally takes months even years to be cleaned up. Due to the hydrophobic and sorption characteristics, tire rubber powder worked as oil adsorbent. 1 g of 20 mesh rubber powder removed 2.2 g VOC-free motor oil in lab experiment (Lin et al., 2008). The powder could be reused one hundred times without cleaning. Large particle size (40 mesh) and high water

temperature (40 ˚C) decreased the sorption capacity significantly. The cost of rubber powder oil sorbent is three orders of magnitude less than the commercial sorbent Ecosol. The benefits of rubber usage for oil adsorption appear positive. However, the oil-saturated rubber powder needs to be recovered, because it is not biodegradable. Consequently, post-treatment may increase cost, which should be considered carefully.

2.4.3 Toxicity considerations

Although scrap tire rubber has been widely used in many fields as mentioned above, tire rubber toxicity cannot be ignored in these applications. It was pointed out that zinc is leached significantly by tire debris. pH, size, and particles aggregation are major factors influencing the releasing of zinc (Gualtieri et al., 2005). Researchers have found playground and track recycled tires products may release volatile organic compounds (VOCs) and metals causing negative impacts on human health (OEHHA, 2007).

2.4.4 Summary

Reuse and reclaiming of scrap tires have made a progress. Recent research has supported an increase in the market of used tire rubber. However, it is still not sufficient, compared with the increase in tire consumption. More efforts are required

to improve the existing tire reuse technology, to find new applications of tire rubber reuse, and to enhance theoretical research.

2.5 H_2S removal

2.5.1 H_2S in biogas

Biogas is a type of renewable biofuel. Under the anaerobic condition, biogas originates from the biological decomposition of organic matter. The composition of biogas varies with different processes, shown in Table 6.

Table 6. Compositions of biogas (Jenö Kovács, 2007).

Matter	Reactor biogas (%)	landfill biogas (%)
Methane, CH_4	55.0-75.0	54.0
Carbon monoxide, CO	0-0.3	traces
Carbon dioxide, CO_2	25.0-45.0	42.0
Nitrogen, N_2	1.0-5.0	3.1
Hydrogen sulfide, H_2S	0.1-0.5	88 mg/m³
Hydrogen, H2	0-3.0	traces
Oxygen, O_2	traces	0.8

Typically, there are two ways to generate H_2S: anaerobic digestion and biomass gasification. Common biomass feedstock for the former includes sewage, domestic waste, crops, etc., while wood or other biomass is used for the latter. The term given

to biogas produced through biomass gasification is also called syngas. Sulfur is one of important inorganic elements in living cells. In digestion, anaerobic microorganisms used sulfur as electron acceptor for metabolic activities during the digestion process, which results in H_2S release. In gasification (pyrolysis), H_2S is also generated because sulfur is reduced to S^{2-} in the uncompleted combustion process in the absence of oxygen. The removal of H_2S is beneficial use of the biogases.

2.5.2 Control technology for H_2S in biogas

Many strategies have been developed to remove H_2S from biogas, including inhibition of H_2S formation, chemical scrubber, biological scrubber, membrane, and adsorption.

2.5.2.1 Inhibition of H_2S formation

H_2S is the reduction product of elemental sulfur or higher valence sulfur compounds, such as sulfate, by microorganisms or by chemical reaction. If the sulfur or sulfide could be oxidized or if the reduction process in the reactor is inhibited, the production of H_2S would be controlled to a low level. In this section, chemicals or bacteria are discussed.

Sodium molybdate is one type of chemical inhibitors. It competes with sulfate as an electron acceptor in a digester bioreactor. However, sodium molybdate might cause environmental pollution. Consequently, if molybdate is present, a second treatment of molybdate removal is necessary (Ranade et al., 1999). Another problem is that a high

dose of molybdate also inhibits methanogenic activity and decreases the heat value of biogas.

Compared with the chemical inhibition method, a biological inhibition causes less secondary pollution and is cheaper. By using sulfur bacterial in the anaerobic bioreactor with low amount of oxygen, the sulfide would be oxidized to elemental sulfur, thiosulfate, and polysulfide (Van der Zee et al., 2007). Consequently, it would decrease the generation of H_2S. But the reappearance of sulfide is possible if the oxygen is completely consumed in the consequent treatment. Therefore, it is important to keep the oxygen lever in the application of this method. Iron-oxidizing bacteria have a similar mechanism to remove H_2S indirectly. Some researchers emphasized that the carrier matrix of bacteria and the type of bioreactor are also important and recommended that the combination of polyurethane foam in immobilized bioreactors is an effective and practical choice (Park et al., 2005)

2.5.2.2 Chemical scrubbers

Chemical reactions dominate the scrubbing mechanism of H_2S. It could be a dry sorption process or liquid process.

Metal oxides are common H_2S adsorbents and many of them has been developed as commercial products: e.g. Sulfatreat 410-HP®. For these systems, iron oxides (Fe_2O_3, Fe_3O_4) are active components. The adsorption behavior of the adsorbent was investigated and developed as a preliminary kinetic model (Truong and Abatzoglou, 2005):

$$-r_{A=0.0243C_A^{0/935}C_B^{0.03}}$$ Equation 6

Here, $-r_A$ is the reaction rate; C_A and C_B are the concentration of H_2S and reactive sites consumed, respectively. The empirical model suggested the reaction is close to first order for the H_2S concentration and zero order for the adsorption media.

ZnO powder adsorbs H_2S in steam by following the reaction:

$ZnO(s) + H_2S(g) = ZnS(s) + H_2O(g)$

under higher temperatures of 300~375°C (Novochinskii et al., 2004). Large surface areas and lower temperatures benefitted the removal process while higher water content would drive the reaction back to ZnO and H_2S, which decreased the removal of H_2S.

In solution, metal oxides work as a scrubbing media as well. Aqueous solutions of ZnO and CuO were investigated. Both qualified as scrubbers, and CuO had a higher adsorption capacity (Haimour et al., 2005). They fitted the experimental data of H_2S with Langmuir, Freundlich, and Redlich-Peterson isotherm models. Both the Langmuir and Redlich-Peterson models showed a better fit for the CuO experiment while the Redlich-Peterson isotherm is better for ZnO.

Freundlich isotherm:

$$q_{e=K_F C_e^n}$$ Equation 7

where q_e is the sorbate concentration on sorbent; C_e^n is the sorbate concentration in solution; K_p is the partition coefficient.

Redlich-Peterson isotherm:

$$q_e = \frac{aC_3}{1+bC_s^{\beta}} \qquad \text{Equation 8}$$

where the parameters a, b, and β can be determined by non-linear regression analysis of the experimental data using a non-linear program.

2.5.2.3 Biological scrubbers

Biological scrubbing methods also take advantage of the oxidation of H_2S, but in this case oxidation is performed by microorganisms. Sulfur oxidation microorganisms could be fixed on films in a H_2S bioscrubber or biotrickling filter; this approach use in contact columns as shown in Figure 5. This design benefits the continuous operation of H_2S removal and nutrition supply for microorganism growth by recycling nutritious liquid. By controlling the contact time, inlet gas rate, and nutrition liquid flowrate, the removal efficiency could attain 98% (Potivichayanon et al., 2006).

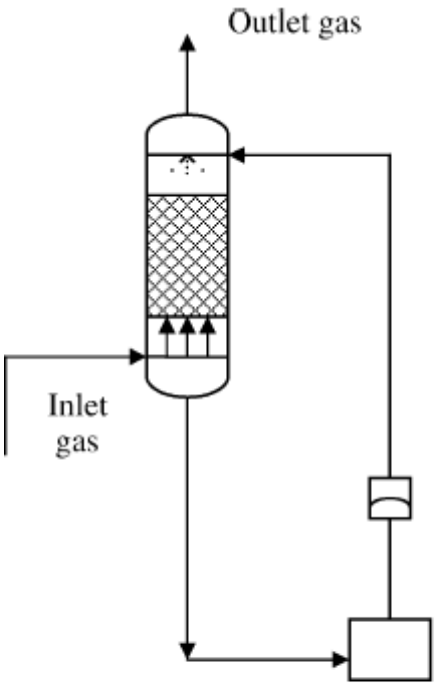

Figure 5. Schematic diagram of the fixed-film bioscrubber (Potivichayanon et al., 2006).

A biotrickling filter pilot experiment under anoxic conditions was conducted with specific bacteria such as *Thiobacillus denitrificans*, following the reaction (Soreanu et al., 2008):

$$H_2S + CO_2 + \text{Nutrients} + NO_3^- \xrightarrow{\text{Microorganisms}} \text{Cells} + S / SO_4^- + H_2S + NO_2^- / N_2$$

The removal efficiency could reach > 99% with an capacity of 270–300 g $H_2S/(m^3\text{biofilter}\cdot\text{day})$.

2.5.2.4 Adsorption

Adsorption is a chemical-physical process, including complex mechanisms, such as diffusion, mass transfer, catalysis, reaction, etc.

Activated carbon is a type of ideal adsorbent with large surface area, high porosity, and surface catalysis. Numerous studies evaluated the mechanisms, adsorption kinetics, and adsorption equilibrium of activated carbon. The surface characteristics of activated carbon, such as specific surface area, pore size, moisture content, pH, and surface chemistry (oxygen containing functionalities), might influence the adsorption of H_2S. These functionalities are chemical functional groups, such as carboxyl, anhydride, lactone, and phenol groups. Normally, high specific surface area provides a larger capacity for H_2S attachment to the adsorbents. It was reported that an optimized combination of moisture, pore size, and surface chemistry parameters increase the adsorption capacity (Bagreev and Bandosz, 2001). They argued that moderately low pH would promote the oxidation of H_2S. Surface chemistry and porosity significantly were found to contribute to the removal of H_2S (Bandosz, 1999). Heterogeneous activated carbon with micro- and mesopores performed better than predominantly microporous materials even with high surface areas. The activated carbon resulted in the adsorption of water, which takes an important role in the H_2S oxidation. Impregnated activated carbon shows a better adsorption capacity compared with virgin activated carbon. Caustic materials are supposed to impregnate in activated carbon since H_2S is a kind of acidic gas. NaOH or KOH could increase the adsorption capacity significantly (Tsai et al., 2001). They determined that

impregnated NaOH could increase the adsorption capacity up to five times, which can be attributed to chemical reactions because the surface area decreases after impregnation. Other weak bases could enhance the removal efficiency, such as Na_2CO_3. Impregnated chemicals can change the surface properties and enhance the chemical reaction between activated carbon and H_2S (Xiao et al., 2008), using the following equation:

$$H_2S(g) + Na_2CO_3(s) \rightarrow NaHS + NaHCO_3$$

Higher humidity could benefit the reaction. They also reported that the adsorption equilibrium of Na_2CO_3 impregnated activated carbon fits the Langmuir isotherm model and the adsorption behavior was dominated by intraparticle diffusion. Despite all the research focusing on the activated carbon adsorption of H_2S, the adsorption of H_2S by virgin or by caustic impregnated activated carbon proceeds by different mechanisms, which are not yet fully understood (Adib et al., 1999). It is believed that H_2S is ionized in the water film and oxidized by oxygen radicals to sulfur oxides on virgin activated carbon, but H_2S reacted with the base before oxidation on the caustic activated carbon. The oxidation proceeded as follows (Bagreev and Bandosz, 2000),

$$C_f + H_2S \leftrightarrow C(H_2S)_{ads} \text{ (adsorption)}$$

$$C(H_2S)_{ads} + H_2S \leftrightarrow C(S_xH_y)_{ads} \text{ (polysulfide formation)}$$

$$C_{ox} + H_2S \leftrightarrow C_{red} + S^\circ + SO_x + H_2O \text{ (surface reaction)}$$

where, C_f is a free active site on the carbon surface; C_{ox} is a surface oxygen group; and C_{red} represents the product of the reduction of that group.

Sludge-derived H_2S adsorbents have attracted research recently. Although the surface area is lower than activated carbon, the heavy metal in sludge could produce more chemical active sites contributing to the removal of H_2S. Metal sludge from the galvanizing industry was used as an adsorbent precursor (Yuan and Bandosz, 2007). They found the capacity of removal was comparable with activated carbon. Pyrolysis temperature and metal composition influenced the performance of the adsorbent, because these factors decide the distribution and amount of chemical activated sites. Water enhanced the process by providing a reaction medium for H_2S oxidization. Sewage sludge was another type of H_2S adsorbent precursor. It is a potential market for the sludge disposal. Fly ash was found to have a more detrimental effect on the sludge-derived adsorbent, because the ash decreased the porosity and hydrophilicity (Seredych et al., 2008).

Molecular sieves, such as Lime (mineral), Silica gel, and Zeolite, are a type of common high capacity adsorbent because of the tiny pores on it. Molecular sieves can separate the gas or liquid by molecular size. Zeolites are microporous, aluminosilicate minerals. The three-dimensional pore system of the crystals has a similar size as H_2S molecular, which allows H_2S to be adsorbed in the pores. The adsorption mechanism of HZSM5 (Si/Al = 35.5) Na-ZSM5 zeolites of H_2S were investigated (Garcia and Lercher, 1992). HZSM5 Zeolite was found to hydrogen bond H_2S by the unique interaction with - SiOHAl surface groups while Na-ZSM5 zeolite

adsorbed H_2S by substituting a Na element for the S element of H_2S. They also pointed out that H_2S may have undergone oxidation, since water was detected as a product of the experiment. The water produced would agree with the following equation:

$$H_2S + (1/2)O_2 = H_2O + S$$

2.5.2.5 Membrane

Membrane methods are not new. However, with the improvement of membrane technology, the separation of H_2S from biogas is more economical and effective. Polyelectrolyte membranes contain high ion content which provides a large number of reaction sites to remove acid gas, such as CO_2 and H_2S. On the other hand, the membrane allows methane and hydrogen gases to permeate. Poly-vinylbenzyltrimethylammonium fluoride (PVBTAF) membranes were used to separate acid gases from methane or hydrogen (Chatterjee et al., 1997). H_2S can react with the ion on the membrane and be removed according to the following equation:

$$2F^- \bullet nH_2O + H_2S = HS^- + HF_2^- \bullet 2nH_2O$$

The key to membrane separation is to increase the H_2S/CH_4 sensitivity. The poly(ether urethane urea) PU4 synthesized by some researchers is a type of high H_2S/CH_4 selectivity membrane which can reduce the H_2S concentration down to 4 ppmv (Chatterjee et al., 1997). However, the membrane cannot handle a high H_2S concentration steam. Pretreatment is required to couple to this method. Most biogas

or natural gas purification includes both H_2S and CO_2. However, the CO_2/CH_4 selectivity is normally much higher than H_2S/CH_4 selectivity. It negatively affects the simultaneous removal of both acid gases. It was reported that the two-stage poly membrane process with CO_2-selective membranes in the first stage before H_2S-selective membranes could improve the removal of H_2S in the second stage (Hao et al., 2002). Although they did not find impressive improvement, it still provides a potential solution to the problem.

2.5.2.6 Other methods

One simple oxidation method is pumping oxygen/air into biogas to oxidize H_2S into sulfur,

$2H_2S+O_2 = 2S+2H_2O$

The low cost method could remove 95% H_2S to less than 50 ppmv (Kapdi et al., 2005). This method is suitable for higher H_2S concentration biogas. The procedure is also affected by the temperature, reaction time, and the amount of methane in biogas.

Recently, electrochemistry was also induced as a removal option for H_2S. The advantage of this method is the generation of hydrogen from H_2S:

Anode electrolysis: $H_2S \rightarrow 2H^+ + 2e^- + 1/8S_8$

Cathode electrolysis: $2H^+ + 2e^- \rightarrow H_2$

A thin, solid-state membrane H_2S electrochemical cell was created following the theory (Mbah et al., 2008). Although the lab experiment successfully spit H_2S into sulfur and hydrogen, the interferences of other gases should be considered in filed application.

2.5.3 Summary

Among the H_2S control methods, it is hard to assert which one is most suitable. Technical, economical, social, and environmental factors should be considered comprehensively to find a final solution for H_2S removal. Due to the low cost of adsorption, combined with the simple operation and low facility investment, the adsorption method is still a promising technology. However, the adsorption mechanism varies with different adsorbents and the mechanism is not clear even for well-studied adsorbents like activated carbon. More research is necessary since an understanding of the mechanism would result in an improvement of adsorption capacities.

CHAPTER 3. MATERIALS AND METHODS

The research work was divided into two experiments—the characterization of TDRP™ samples and the evaluation of the H_2S adsorption mechanism. The purpose of firs experiment was to find the possible components or properties in TDRP™ relating to H_2S adsorption. All the potential properties relating to H_2S adsorption were detected. The aim of the second experiment was to test these possible factor's effects on the adsorption capacity to investigate the mechanism.

3.1 Characterization of physical and surface properties of TDRP™

3.1.1 Bulk density and particle density

In order to measure bulk density, a beaker with a volume 140 mL was filled with TDRP™ and ORM™ separately. The weight difference before and after filling was recorded as W. Consequently, the bulk density without compressing was calculated by equation: W/140 mL.

In order to evaluate particle density, a 0.5 g TDRP™ or ORM™ sample was placed into a 50 mL tube without shaking. A measured mass of TDRP™ or ORM™ sample was combined with known volume of water and allowed to sit at room temperature for 24 h. Glass tubes with stoppers were used as containers. When all the samples settled on the bottom, the tube was filled with water and the total volume of water was measured as V1. After the tubes were cleaned and dried, the volume V2 of tube was measured with water. Consequently, the particle density was calculated by Mass/(V2-V1).

3.1.2 Moisture content

In order to measure the moisture content, two beakers were heated under 105 ˚C for 4 h and then cooled in a dessicator to room temperature. The beakers were weighed and the procedure was repeated until the weight change was less than 0.1 g. The next step was to transfer about 10 g ORM^{TM} and TDRP^{TM} into the breakers separately. Then, the samples were weighed and transferred to the oven at 105˚C for 8 h. Next, the samples were cooled in the dessicator to room temperature and weighed again. This process was repeated once more. Moisture content was calculated by the following equation:

(W TDRP^{TM}/ORM^{TM} and breaker-W Dry TDRP^{TM}/ORM^{TM} and breaker)×100 %/(W TDRP^{TM}/ORM^{TM} and breaker –W Breaker)

3.1.3 Thermogravimetric analysis (TGA)

Thermogravimetric analysis (TGA) was used to estimate the carbon black concentration of TDRP^{TM} and ORM^{TM}. Approximately 40 mg of a TDRP^{TM} or ORM^{TM} sample was placed into a TGA analyzer (PerkinElmer T6A7) and heated from 50 ˚C to 650 ˚C at 5 ˚C/min. Nitrogen and air of volume ratio 1:1 were used as carrier gas. The composition concentration were then be estimated by the inflections of mass curve.

3.1.4 Surface pH

To measure the surface pH, 4 g TDRP™ or ORM™ was added to 50 mL water and shaken for 12 h. After filtering the TDRP™ or ORM™ particles, the rinsing water's pH was tested with Accumet XL15 pH meter. The procedure was repeated for three times to get average values. A blank sample was used to test the background pH of distilled water.

3.1.5 Infrared test

Raw and H_2S-saturated TDRP™ samples were sent to Dr. Steven Martin for the IR test in the Department of Materials Science and Engineering at Iowa State University.

3.1.6 Mass spectra test for H_2S-saturated ORM™

H_2S-saturated ORM™ samples were sent to chemist James Anderegg in Ames lab to evaluate using mass spectra tests. Under different temperatures, the release of gases of the sample was monitored by MS detector.

3.1.7 BET surface area

The nitrogen adsorption method was used to test surface area and pore size of TDRP™ or ORM™. Roughly a 50 g sample was heated in an oven at atmospheric pressure at 120˚C for 48 h to remove volatile compounds. Then, the samples were

evacuated at 100 ˚C (temperature rises to 100 ˚C at rate 10 ˚C; Evacuation rate is 30.0 mmHg/s; Evacuation time is 300 min; Vacuum set point is 10 um Hg). The nitrogen adsorption isotherm was found at 77 K. Then, the data were analyzed by the ASAP 2020 BET Micromeritics for BET surface area and BJH pore size calculation.

3.1.8 Surface oxidation functionalities of TDRP™ and ORM™ (Boehm Titration)

Boehm established a classic theory to estimate the oxidation group concentration on the surface of some materials (Boehm, 1966). In the theory, $NaHCO_3$ neutralizes carboxylic groups; Na_2CO_3 neutralizes carboxylic groups and also allows lactonic groups to open and form carboxylic groups, which are then neutralized; NaOH neutralizes carboxylic, lactonic, and phenolic groups. Titrations and differences between titrations allow for estimation of the number of carboxylic, lactonic, and phenolic surface groups. In the experiment, the method "Boehm Titration for carbon black" was employed, and it was assumed that carbon black occupies a large proportion in tire rubber particles. A sample of 0.25 g TDRP™ or ORM™ was added in test tubes, and each tube contained either 0.05 M $NaHCO_3$, 0.05 M Na_2CO_3, or 0.05 M NaOH. After shaking for 24 h, 10 mL samples were filtered and transferred to 100mL beakers. A known excess volume of 0.05 M HCl and 4 drops of Phenolphthalein were then added to the solution. Finally, 0.05 M NaOH was used to titrate the solution until the solution's color changed to pink.

3.1.9 Metal concentration

TDRP™ and ORM™ samples were sent to Minnesota Valley Testing Laboratories, Inc. (MVTL) for metals analysis. MVTL used digestion followed by Inductively-Coupled Plasma (ICP) with Atomic Absorption (AA) to measure the concentrations of calcium, magnesium, copper, iron, lead, silver, and zinc in the TDRP™ and ORM™ samples.

3.1.10 X-ray photoelectron spectroscopy analysis for TDRP™ samples

TDRP™ samples were sent to chemist James Anderegg in Ames lab for XPS analysis. The samples included a raw TDPR sample, an H_2S-saturated TDRP™ sample, an HNO_3-rinsing TDRP™ sample, and an H_2S-saturated HNO_3-rinsing TDRP™ sample. The relative surface concentrations of some elements, carbon, oxygen, sulfur, zinc, and nitrogen were detected.

3.2 H_2S adsorption on TDRP™ and ORM™

An adsorption reactor was made using a clear PVC column connected to H_2S gas cylinder, an air source, and an H_2S sensor. The entire system was placed within a fume hood to ensure safety. The dimensions are shown in Figure 6.

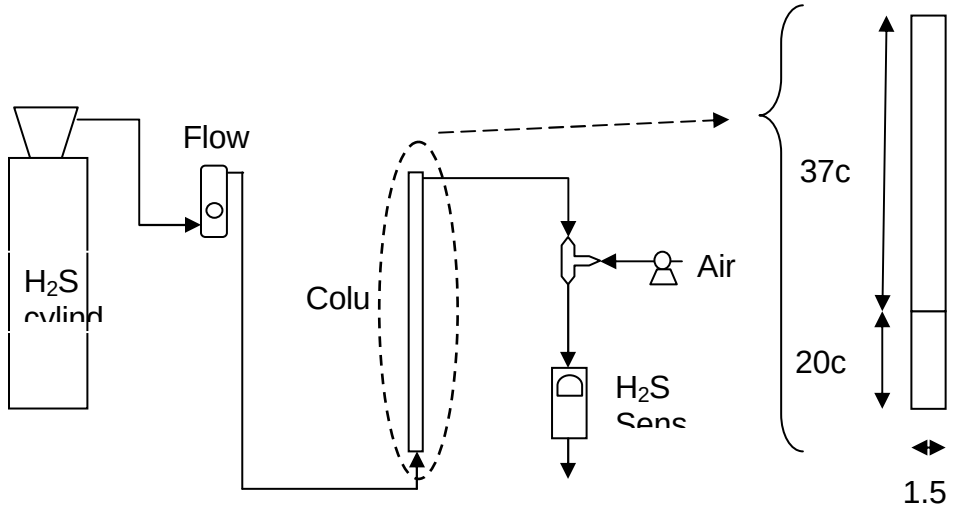

Figure 6. Scheme of H_2S adsorption experiments.

3.2.1 Breakthrough curve

To measure breakthrough curves, first, a 10 g TDRP™ or ORM™ sample was packed into the PVC column. Then, 200 ppmv H_2S (in Nitrogen or Helium) was introduced into the inlet at a flowrate of 0.3 mL/min. To meet the analytical requirements of Jerome 860 H_2S sensor, air was added to the column outlet gas prior to flowing to the sensor. The air flowrate was 0.22 mL/min. Then, the data read from sensor indicated the concentration of the mixture of outlet gas and air. Data measured by the sensor was corrected to the air free H_2S concentration. The experiment was stopped when H_2S sensor read 100 ppmv. TDRP™ and ORM™ samples were tested separately.

3.2.2 Moisture effects

TDRP™ or ORM™ samples were rinsed in water and shaken for 12 h. After drawing most of free water using a pump, the samples were placed in the drying oven for different times from 0.5 h to 2 h at 105 ℃ to provide TDRP™ or ORM™ samples with different moisture contents. For each sample, 10 g ORM™ on a wet basis was used to test H_2S adsorption capacity while the rest was used for moisture content test with the method mentioned. The dried TDRP™ or ORM™ mass was calculated with weight after 16 h heating. The difference between the weights after 8 h and 16 h was used to see if there is some material decomposing under such temperature. The difference was found to be less than 1% suggesting no decomposition.

3.2.3 Zinc effects

TDRP™ samples (20 g) were rinsed in $ZnCl_2$ solutions with different concentrations and shaken for 12 h. After being dehydrated in an oven, the samples were balanced for moisture content in room for 24 h. Then, the samples were used to test H_2S adsorption capacity.

3.2.4 Zinc extraction test

To evaluate the effects of zinc on TDRP™ samples, zinc extraction experiments were designed. Nitric acid and sodium hydroxide solutions were chosen as extractants. A sample of 1 g TDPR type B sample was shaken and rinsed with 100 mL of either 0.1 N, 0.5 N, or 1 N HNO_3, and samples were mixed with NaOH solutions for 24 hours respectively. Then, the mixture was filtered with Büchner funnel and filter paper. The zinc concentration of the filtered solution was determined with GBC 932 plus Atomic Absorption Spectrophotometer (GBC Scientific (USA) LLC.) in Environmental Engineering Research Laboratory of Iowa State University. The solid substances were rinsed again for secondary extraction. The tertiary extraction also was applied. For the AAS test, 10% nitric acid solution was used as for standards, which was made from concentrated nitric acid with trace metal grade reagents (Thermo Fisher Scientific Inc.). Then, nitric acid was added to all the liquid until a concentration of 10% was achieved. A calibration curve was made with 1 ppmw, 5 ppmw and 10 ppmw zinc solutions, which were diluted from 1000 ppmw zinc oxide standard solution (Thermo Fisher Scientific Inc.).

The 50 g TDRP™ samples were rinsed with 1 L of 0.1 N and 0.5 N nitric acid and sodium hydroxide solution for 24 hours respectively. After filtration, the solid was heated at 105 ˚C for 24h and balanced in air for another 24h. Then, the samples were used to test H_2S adsorption capacity. A representative gas with 200 ppmv H_2S (in helium, purchased from Matheson Tri-Gas, Inc.) was used. The H_2S gas was introduced into the inlet at a flowrate of 0.3 mL/min. The breakthrough test used was

the same as described in section 3.2.1 except the breakthrough concentration used was 80 ppmv.

3.2.5 Particle size effects

In order to evaluate the relationship between surface area and sorption capacity, thereby differentiating adsorption from absorption, the samples were sieved into specific size fractions prior to evaluating H_2S removal. TDRP™ and ORM™ samples were sieved as three classes by radius: less than 0.6 mm, between 0.6 mm and 1 mm, and larger than 1 mm. The sieved sample was used to test H_2S adsorption capacity by following the procedure in section 3.2.5.

CHAPTER 4. RESULTS AND DISCUSSION

4.1 Characterization of physical and surface properties of TDRP™ and ORM™

4.1.1 Density and moisture content

Density and moisture test results are shown in Table 7. The table shows the low bulk density of both TDRP™ and ORM™. The particle density of unground tire rubber is typically between 0.83 and 0.96 g/mL (Colom et al., 2007, Bignozzi and Sandrolini, 2006, Hernandez-Olivares et al., 2002), which is close to the density of water. The densities of TDRP™ and ORM™ samples are slightly greater than this, as shown in the table. It is possible that additives, such as metal and carbon black, contributed to the variability in the density. Furthermore, different brands of tires may have different compositions which could all be used as raw materials for the manufacture of TDRP™ and ORM™. It was reported that the bulk density of tire rubber particles is 0.285 kg/m^3, which is similar to the results from these experiments (Purakayastha et al., 2005). Compared with bulk density, particle density is less useful in field utilization. The former is helpful to determine the volume of TDRP™ and ORM™ adsorbent when in the H_2S scrubbing unit.

Table 7. Density and moisture of TDRP™ and ORM™ samples.

Item	ORM™	TDRP™
Bulk density (kg/m^3)	0.21	0.31
Particle density (kg/m^3)	0.95±0.06[A]	1.28±0.13
Moisture content (%)	1.31±0.004	0.56±0.003

[A]Mean±Standard Deviation

Based on the low background moisture content, as shown in Table 7, TDRP™ and ORM™ do not freely sorb water from air. When TDRP™ and ORM™ samples were rinsed in water, all samples floated on the surface of water at the beginning. However, after being shaken for three days, all the particles settled on the bottom of tube. The phenomenon means the TDRP™ and ORM™ samples' particle density may be heavier than water or close to it, which matches the particle density test results.

According to studies on the H_2S adsorption mechanism on the surface of activated carbon, water plays an important role in the oxidation of H_2S (Bouzaza et al., 2004, Bagreev and Bandosz, 2001). They showed that adsorption capacity of H_2S decreased sharply without water. Water may provide a favorable environment for H_2S oxidized by free radicals or reacting with other chemicals. It is thought that the first step of adsorption is that the H_2S dissolves in the water on the surface of the adsorbent. The low moisture might be the limiting step or reactant for the adsorption of H_2S.

4.1.2 Thermogravimetric analysis (TGA)

Tire rubber, which is the raw material of TDRP™ and ORM™, is made of carbon black, polymer, and other trace elements (silicon, sulfur, chlorine, etc) (Williams and Besler, 1995). Polymer adsorption was not found in literature or previous work, while carbon black was proved to adsorb gases, which may contribute to the H_2S adsorption on TDRP™ and ORM™ samples (Rodgers, 2004). The concentration of carbon black was estimated by TGA analysis. The rubber would show a typical TGA with two weight losses: the first one related to the polymer decomposition and the second one due to the carbon black oxidation (Williams and Besler, 1995). The concentrations of carbon black were found to be about 45.6% for ORM™ and about 47.8% for TDRP™ (TGA curves shown in Appendix-Figures 1a and 2a). The concentrations are higher than commonly described for tire rubber (around 20–35%) (Dave, 2009). Many researchers (Manchon-Vizuete et al., 2005; Pantea et al., 2003; Hamadi et al., 2001) claim tire derived carbon black inherently contains a high adsorption capacity. For TDRP™ and ORM™, carbon black may provide a large surface area for adsorption and oxygen containing functionalities to oxidize H_2S. As mentioned above, large parts of pores and functionalities are occupied by polymer during the tire rubber production. However, it is possible that active sites are created by abrasion and oxidation in air while the rubber from TDRP™ was in service. The TGA test results show TDRP™ and ORM™ samples are stable at temperatures up to 250 ˚C. Therefore, TDRP™ and ORM™ could be used to remove H_2S from gas steams at elevated temperature from other industrial processes.

4.1.3 pH

Low pH is unfavorable H_2S adsorption, which has been shown with activated carbon research (Adib et al., 1999). The surface pH of TDRP™ and ORM™ samples were both higher than 7, as shown in Figure 7. If the adsorption mechanism of TDRP™ or ORM™ was similar to activated carbon, the moderate higher pH would enhance the adsorption of H_2S. One reason for the higher pH values may be because some alkaline chemicals were added during the TDRP™ and ORM™ production process. Another reason may be that some metal element exists in the form of oxides, e.g. ZnO (Smolders and Degryse, 2002), which increase the pH of water when dissolved.

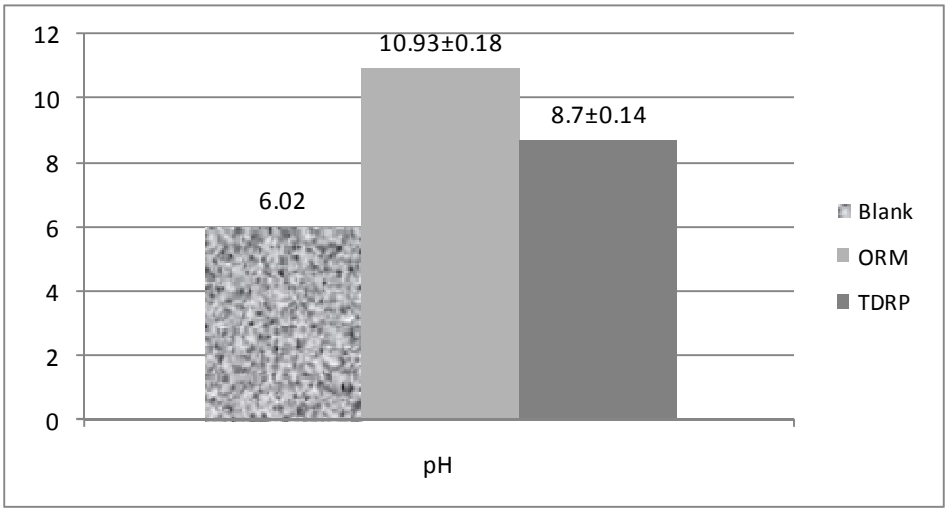

Figure 7. Surface pH of TDRP™ and ORM™.

4.1.4 Surface characterization

Surface area and pore size measurements are shown in Table 8 as measured by the micrometrics analysis. According to the pore size of TDRP™ and ORM™ samples, they should be defined as a mesoporous material. However, other mesoporous materials with a pore size near 10 nm normally have a surface area of several hundred m^2/g (Alonso-Lemus et al., 2009). The low measurement for surface area suggests the data about pore size are not reliable, and TDRP™ or ORM™ are possibly only particle materials rather than porous materials. It might mean physical adsorption is less meaningful.

Table 8. BET surface area and pore size of TDRP™ and ORM™.

Item	ORM™	TDRP™
BET Surface Area (m^2/g)	0.280	0.226
BJH Desorption average pore diameter Å	143.327	71.128
BJH Adsorption average pore diameter Å	68.028	90.114
H_2S adsorption capacity/specific surface area (mg/m^2)	3.569~10.707	4.431~13.291

As a comparison, the BET surface area and pore size of activated carbon are about 1200 m^2/g and 10 Å, respectively, and the breakthrough capacity varies from 5 to 300 mg/g (Adib et al., 1999; Bandosz, 1999). The adsorption capacity of TDRP™ and ORM™ (1~3 mg/g) is smaller than the capacity listed for activated carbon, but, it should be noted that the ratio of H_2S adsorption capacity to specific surface area for TDRP™ or ORM™ is higher than for activated carbon. This suggests that the

mechanism of TDRP™ or ORM™ is perhaps different from the adsorption mechanism for activated carbon. The surface capacity may be higher because the contact time used is longer, or TDRP™ or ORM™ adsorb with chemical reactions; e.g. metal-hydrogen sulfide reaction.

From the IR spectrum (Shown in Appendix - Figure 3a), TDRP™ and ORM™ may contain carbon dioxide or carboxyl functional groups based on the peaks measured at 2400 cm^{-1}. After saturation of H_2S, a H_2S peak was not found in IR spectrum for TDRP™ and ORM™ samples. Several reasons are considered:

- It is possible that the H_2S concentration was too low to be detected
- H_2S reacted and the sulfur species changed to a form which was not detected by IR spectrometry
- H_2S was adsorbed within pores and covered so that it was inaccessible by the IR beam.

Boehm Titrations were performed to evaluate the surface function groups on TDRP™ and ORM™. The titration results, (Shown in the Appendix-Table 7a), do not fit Boehm's theory for surface functional group titration. The data depicts an unusual relationship between the titrations. Sodium hydroxide should consume a greater volume of titrant, because more surface functionalities are affected by sodium hydroxide than the other two chemicals. The mass of TDRP™ and ORM™ were increased and the tests were repeated in an attempt to obtain repeatable results. The titration results (Shown in the Appendix-Table 8a) show the concentration of oxidation functional groups was still lower, as shown in Table 9.

Table 9. Oxidation functionalities concentrations of TDRP™ and ORM™ by Boehm Titrations.

Item	ORM™	TDRP™
Carboxylic group conc. (mol/g)	0.0018	0.0027
Carboxylic and lactonic groups conc. (mol/g)	0.0029	0.0031
Carboxylic, lactonic and phenolic groups conc. (mol/g)	0.0001	0.0000

Therefore, it is possible that Boehm theory does not work here. But, it still provides some information; based on the measured combined concentrations of surface groups (using hydroxide), the concentration of total oxidation functional groups is lower than activated carbon. The low concentration matches the higher pH of 8.56 to 11.53 versus 4.04~5.6 of virgin activated carbon (Adib et al., 1999; Boudou et al., 2003). Depending on acid-base balance theory, a higher surface pH better supports adsorption of H_2S on the surface of TDRP™ and ORM™. The unusual Boehm titration results increases the suspicion that some chemicals interfere with the experiments, e.g. metal ions.

4.1.5 Metal content

The metals test results are shown in Table 10. Zinc, magnesium, and iron persist in the TDRP™ and ORM™ in high concentrations based on the sample analysis. Most of the metal elements exist in the form of metal oxides. Perhaps, this is the reason for the increase in pH of water solution measured during that pH test. Additionally, the

formation of metal hydroxides resists the reaction with NaOH much more than $NaHCO_3$ and Na_2CO_3, which would explain the Boehm titration results. With a higher pH, metal carbonates easily form. If this is true, the surface acid functional groups concentration information provided by the experiment is not reliable since most reactions happen between metal and sodium compounds rather than acid functionalities and sodium compounds. Furthermore, most oxidized metal elements found are common H_2S scrubbers. This supports the hypothesis that the primary mechanism of H_2S adsorption is chemisorption.

Table 10. Metal test result of TDRP™ and ORM™.

Metal	ORM™ Concentration (mg/Kg)	TDRP™ Concentration (mg/Kg)
Calcium	1.4	2812.0
Magnesium	5017.0	483.0
Copper	0.5	7.0
Iron	269.4	1512.0
Lead	<6.8	6.8
Silver	---	<0.5
Zinc	17950.0	14220.0
Total	---	---

*The values are calculated by assuming the products are metal sulfides.

4.2 H_2S adsorption on TDRP™ and ORM™

4.2.1 Breakthrough capacity of TDRP™ and ORM™

The results of breakthrough capacity tests for TDRP™ and ORM™ (Shown in the Appendix-Figure 4a) show ORM™ contains a higher specific capacity than TDRP™; although the specific surface area of the TDRP™ sample is higher than ORM™ sample. One explanation is that TDRP™'s surface pH is lower than the surface pH of ORM™. According to analysis of TDRP™, the lower surface pH environment may resist the H_2S adsorption on the TDRP™ and ORM™ surface. The surface pH test results show that pH of TDRP™ is lower than ORM™, which matches the H_2S adsorption capacity comparison. Another possibility is that the moisture content of TDRP™ was lower than ORM™.

.The H_2S scrubbing capacity is shown in Figure 8.

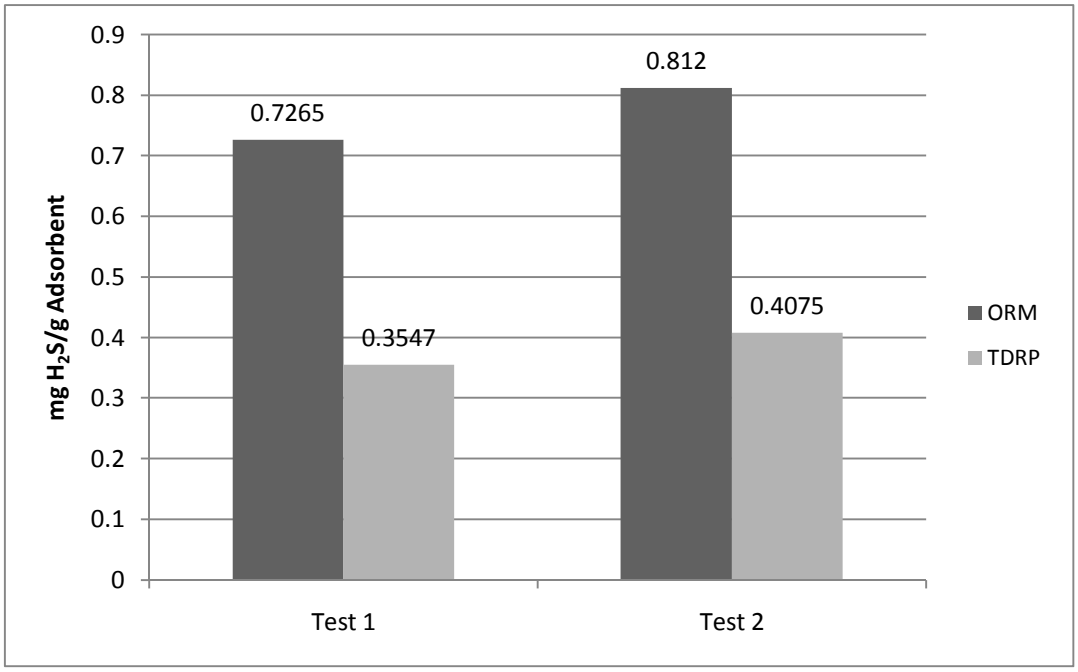

Figure 8. H_2S adsorption capacity of TDRP^{TM} and ORM^{TM}.

4.2.2 Effect of surface area

The size distributions of TDRP^{TM} and ORM^{TM} were analyzed by previous research (Ellis et al., 2008), as shown in Figure 10a. Using these results, the weight proportions of three size ranges (0~0.6 mm, 0.6~1 mm, and 1~ mm) were found. The distribution of ORM^{TM} is more uniform than the distribution of TDRP^{TM}. Appendix-Table 13a shows the H_2S adsorption capacity of TDRP^{TM} and ORM^{TM} samples in different ranges. For both samples, is the adsorption capacity increases as the radius decreases. This can be explained by the different specific surface area of each size group. Small particles have a larger surface area. As Figure 9 shows, the adsorption

capacity shows a correlation with the specific area (m^2/m^3) assuming spherical particles. However, the line cannot pass the origin of coordinates, which means the rubber particles were not an ideal sphere. This could be attributed to the fracture of rubber particles and the irregular shape, which was shown in the SEM (Appendix-Figure 9a) pictures taken by previous research. In this experiment, the TDRP™ and ORM™ samples were sieved with dry method to avoid the water interference on the H_2S adsorption. Unfortunately, the ORM™ has a fiber-like appearance and small particles were easily trapped when dry sieving. This could result in a more uniform specific surface for the three radius ranges; especially the larger radius portion. On the contrary, TDRP™ shows no trapping effect while sieving. The larger radius samples have a lower adsorption capacity than small particles. To check the result of size distribution experiments, the theoretical adsorption capacity of a mixed sample was calculated for both TDRP™ and ORM™ samples. It was the sum of three adsorption capacity multiplied by the weigh percentage of raw sample. The calculated result of TDRP™ sample was similar to the experimental data of a raw sample that was not sieved. On the other hand, ORM™ data showed some differences with the experiment. As mentioned before, this may result from the dry sieve method and the fiber-like appearance.

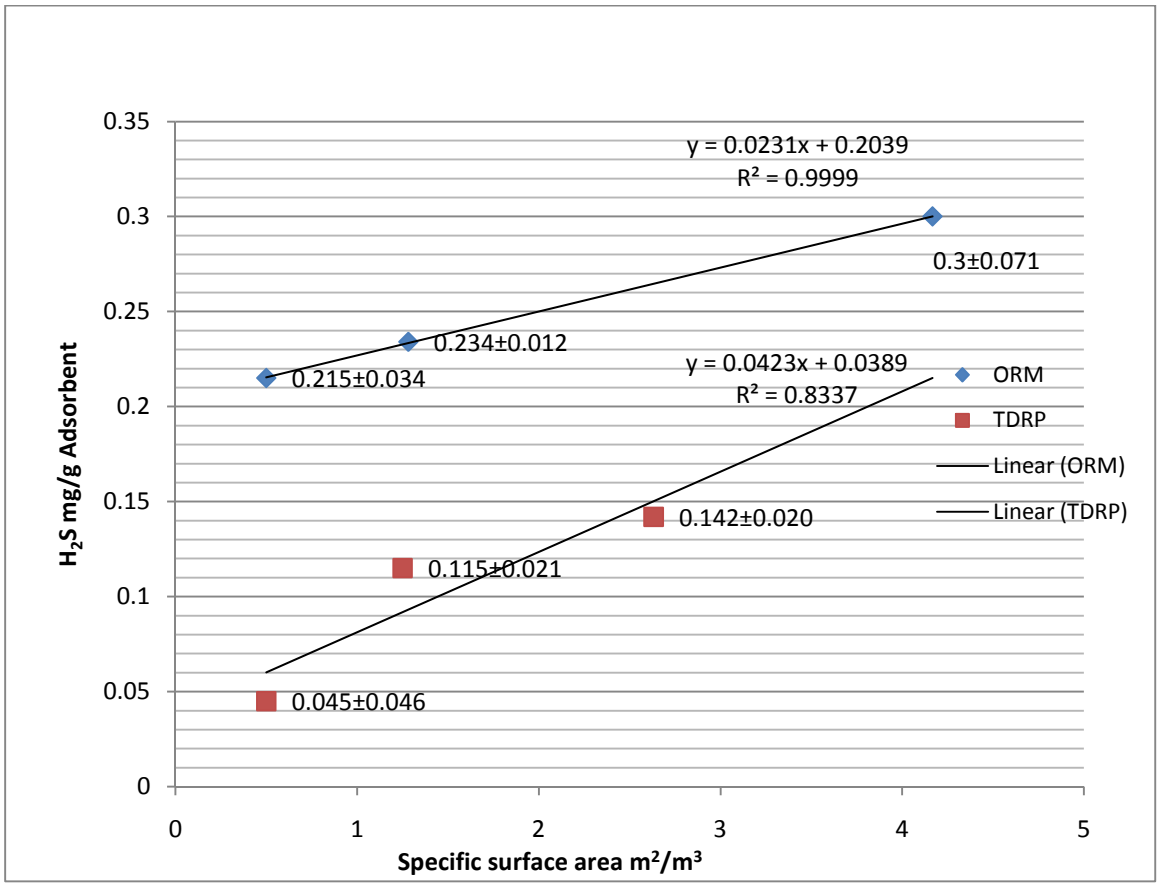

Figure 9. Adsorption capacity of different size of TDRP™ and ORM™ samples.

4.2.3 Effect of moisture content on breakthrough capacity

The adsorption breakthrough curve changes with moisture content. The adsorption capacity of a TDRP™ with a lower moisture content was lower than for TDRP™ with a higher moisture content. The adsorption mechanism may require chemistry reaction in the aqueous phase, which means it needs water to provide a favorable adsorption environment. The fact that H_2S adsorption results (0.13 mg/g) of the dry TDRP™ or

ORM^{TM} sample is much lower than other higher moisture content sample supports the importance of water as a factor in the adsorption mechanism.

Table 11 show the breakthrough time does not change as dramatically as the adsorption capacity does. All curves except the 18.9% moisture content curve tend to breakthrough at the same time. The solubility of H_2S in water at 25˚C is about 3.5 mg/g. This value is lower than the slope, 7.54 mg H_2S/g H_2O, of the line in Figure 10. It means that the increased moisture content is not just a function of H_2S solubility, but water may be a reactant along with other chemicals on the surface of TDRP^{TM} and ORM^{TM}. Similarly, water may be part of the salvation complex, e.g. ZnS*x(H_2O), in precipitation reactions involving H_2S on the surface of TDRP^{TM} and ORM^{TM}.

Table 11. Adsorption capacity of ORM^{TM} with different moisture contents.

	Adsorption capacity (mg/g)	Time to 100 ppmv (min)
Dry ORM^{TM}	0.13	47.2
Moisture content 1.07%	0.73	163.6
Moisture content 1.30%	0.81	180.4
Moisture content 3.8%	0.98	170.8
Moisture content 11.7%	1.67	196.5
Moisture content18.9%	2.07	265.2

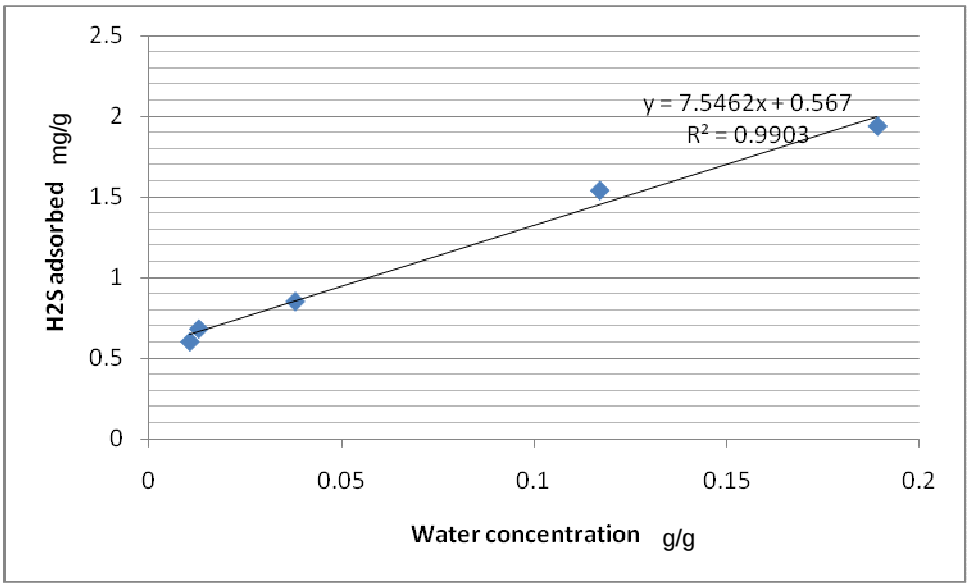

Figure 10. Relationship between H_2S adsorbed and water concentration (subtracting Dry ORM^{TM} H_2S adsorption capacity).

4.2.4 Effect of Zinc on H_2S Adsorption

The zinc concentration of ORM^{TM} was higher than the zinc concentration of TDRP^{TM}. According to the metal test results for TDRP^{TM}, the zinc concentration is 14.22 mg/g, therefore, 7.44 mg/g H_2S could be consumed based on the following equation.

$ZnO + nH_2O + H_2S \rightarrow ZnS^* \; n+1 \; (H_2O)$

Usually, zinc is added after the vulcanization process and works as a wear matrix to accelerate the formation of the rubber polymer (Bandosz, 1999). The theoretical H_2S adsorption is much higher than real amount (1~3 mg/g). It is possible that moisture content contributes to the reaction kinetics and equilibrium if the reaction must take place in the aqueous phase. In another test, $ZnCl_2$ was precipitated on the TDRP^{TM}.

The amount of $ZnCl_2$ added to the TDRP, doubled and tripled the original Zn concentration. The results (Figure 11) show that the adding zinc increases H_2S adsorption capacity on TDRP™ samples. The moisture contents of the samples are not variable (about 1%), which means the adsorption capacity change is not caused by water concentration.

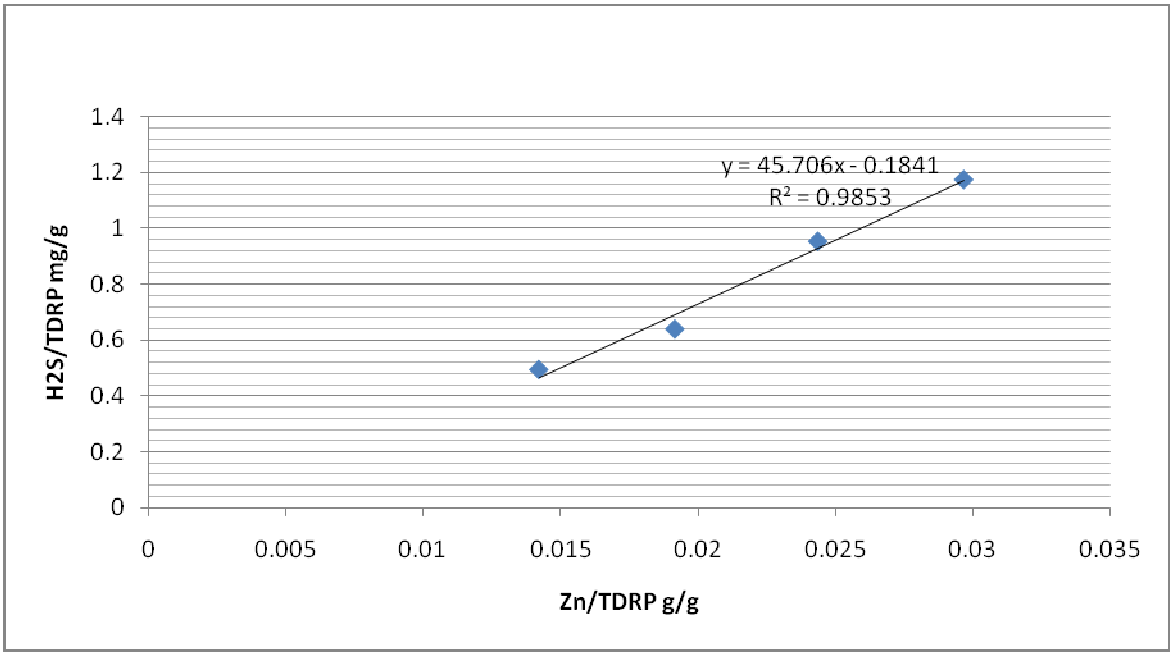

Figure 11. Relationship between H_2S adsorbed and Zn concentration.

One gram of Zn element could react with 520 mg H_2S by stoichiometric calculation of ZnS. As previously mentioned, the original Zn concentration in TDRP™ was approximately 14 mg/g, which translates to an adsorption capacity of 0.7~0.8 mg/g, which is smaller than the experimental value. Furthermore, the zinc concentration includes the fraction of zinc located inside TDRP™ particles, which has no opportunity

to contact with H_2S gas. It means the theoretical value is smaller. These suggest that the Zn reaction with H_2S is not the sole mechanism for removal.

The addition of zinc to TDRP™ samples shows a positive relationship with H_2S adsorption capacity. To confirm the result, the extraction of zinc from TDRP™ samples is necessary. Nitric acid is a common extractant for zinc in rubber material. The AAS results are shown in the Table 12. Based on the data, the extraction efficiency of NaOH and HNO_3 is show in Table 12. The zinc extraction efficiency with both extractants was less than 5% for the primary extraction. This is likely due to the fact that only zinc on surface or near the surface can be extracted easily. Meanwhile, the extraction rates were calculated with the bulk zinc concentration of the entire TDRP™ samples, including the large amount zinc inside the rubber material. The zinc extraction increased with prolonged contact time. As shown in Table 12, the five day extraction resulted in a higher removal than a one day extraction, but the difference was 1.5%.

Table 12. Zinc extraction from TDRP™.

	Zinc extraction efficiency %*			
	Primary extraction	Secondary extraction	Tertiary extraction	Individual 5-day extraction
HNO_3 (0.1 N)	4.0%	0.36%	0.26%	5.52%
HNO_3 (0.5 N)	4.4%	0.36%	0.36%	4.73%
NaOH (0.1N)	1.2%	0.33%		
NaOH (0.5N)	2.1%	0.18%		

* The percentage based on the total zinc amount in TDRP™ detected.

XPS experiment results, presented in Table 13, showed that the surface concentration of zinc changed significantly enough to investigate the zinc effects on H_2S adsorption. Based on these results, a one-day extraction was employed. In addition, the XPS results in Table 13 show that the species of element zinc on the TDRP^{TM} surface has an oxidation of +2, which was assumed to be zinc oxide. It matched the fact that excessive ZnO is usually used as additive in tire rubber manufacture. As shown in Table 12, the NaOH solution removed less zinc than HNO_3. Previous research argue that NaOH can change the structure of zinc stearate molecules (Segre et al., 2002), which may affect adsorption. According to the results, different extractant concentrations also influenced zinc removal efficiency.

Table 13. Atomic Concentrations.

TDRP^{TM}	C 1s	N 1s	O 1s	S 2p	Zn 2p3	Total
Raw	89.28	0.20	8.53	0.43	1.56	100
After HNO_3 extraction	91.80	0.78	6.53	0.12	0.77	100
H_2S saturated	91.00	0.40	6.68	0.21	1.71	100
H_2S saturated after HNO_3 extraction	89.07	1.22	8.52	0.19	1.00	100

The results of H_2S adsorption capacity testing of TDRP^{TM} treated by HNO_3 and NaOH extraction are shown in the Figure 12. The data show a negligible change in the adsorption capacity of the HNO_3 treated sample compared to the raw TDRP^{TM} sample. The adsorption capacity of the NaOH treated sample, however, experienced a substantial decrease in adsorption capacity. This does not match the surface zinc concentration order (raw sample>HNO_3 treated sample> NaOH treated sample). The

reason why HNO_3 treated sample adsorption capacity did not decrease as expected may be attributed to the oxidation of surface groups. According to the previous analysis, there are two possible mechanisms for H_2S adsorption, carbon black and metal ions. Given that a 24 h extraction was performed in the extraction experiments and given that the moisture was controlled around a normal value, it is possible that the oxidation of surface groups resulted in an increased capacity for the acid extraction. Although most pores in carbon black are filled by rubber polymer, it is possible that parts of carbon black were exposed to the atmosphere during the experiment. Therefore, in addition to extracting zinc from TDRP^{TM} samples, HNO_3 oxidized the surface of carbon black and increased the number of functional groups. Many researchers have proved that the oxidation of carbon material, such as activated carbon and carbon black, by nitric acid can improve the adsorption of H_2S (Bagreev and Bandosz, 2000).

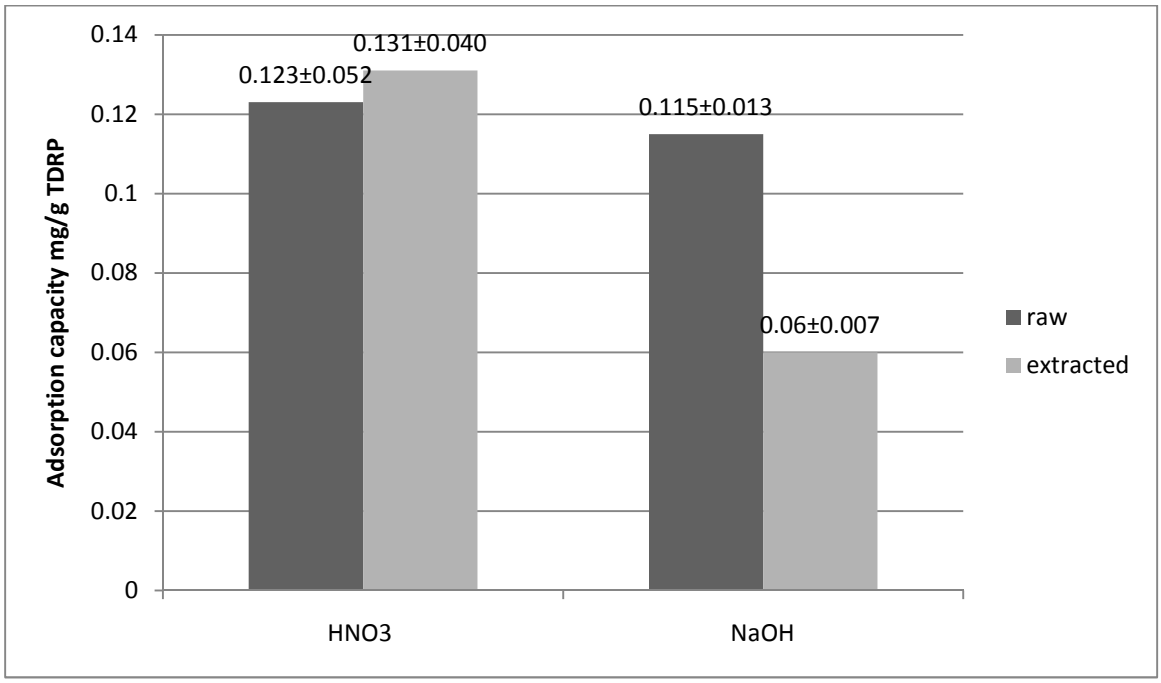

Figure 12. Adsorption capacity of zinc-extracted TDRP^{TM}.

However, the XPS result shows no rise in the oxygen element concentration on the surface of HNO_3 treated TDRP^{TM} sample in Table 13. This could be explained by the reaction occurring between HNO_3 and ZnO as follows:

$$HNO_3 + ZnO \Leftrightarrow Zn^{2+} + H_2O + NO_3^-$$

Parts of the oxygen element were removed from the surface as H_2O and NO_3^-. Then, the balance between an increasing number of surface groups and a decreasing concentration of element zinc may result in the increment of H_2S adsorption capacity on the HNO_3-treated sample. The result of NaOH-treated H_2S supports this conclusion. It is likely that NaOH has a minimal effect on the oxidation of surface groups. Contrary to the results, NaOH-impregnated activated carbon and carbon

black usually increases the adsorption of H_2S. Thus, the effect of NaOH on carbon black can be neglected as a reason why the adsorption capacity declined. Compared with other metal ions, a higher concentration and a higher chemical activity with H_2S make zinc a likely candidate in the adsorption capacity of TDRP^{TM} material.

CHAPTER 5. CONCLUSIONS

By this study, micropores do not dominate the surface of TDRP™ and ORM™. The size range of the pore size, between 2 nm and 50 nm, indicates that TDRP™ and ORM™ should be classified as mesoporous materials. However, TDRP™ has a relative low specific surface area, and the value is much lower than activated carbon and other mesoporous materials. TDRP™ and ORM™ materials are more particle in nature rather than porous. Based on the effects of zinc and moisture content, chemical reaction or chemisorption is the dominant H_2S adsorption mechanism.

Moisture content is essential for H_2S adsorption on TDRP™. Higher moisture contents were shown to enhance the adsorption capacity. This observation further supports the hypothesis that chemical reaction is the main adsorption mechanism because of water is a favorable environment for acid-base reaction.

The pH of TDRP™ is greater than 7. Based on the pH, acid functionalities may not dominate on the surface of TDRP™. Metal oxides may exist on the surface and increase the surface pH. The pH change, however, may not influence the adsorption capacity strongly.

The Boehm titration method was unsuccessful for finding the surface functionalities on TDRP™. Further, it is possible that the metal concentration interfered with the Boehm titrations. According to the data collected, the concentration of oxidation groups is low.

High concentrations of metal elements, such as zinc, were found in the TDRP^{TM} by analytical tests. It is possible that chemical reactions between the metal ion and H_2S are the primary adsorption mechanism. The extraction experiments and component analysis show that the H_2S adsorption on TDRP^{TM} is complex. The overall mechanism consists of some combination of mechanisms due to the different active components, such as zinc and carbon black, in TDRP^{TM}. Future studies are recommended to show how each component affects adsorption, and how the interaction between these components affects adsorption capacity.

5.1 Engineering significance

TDRP^{TM} and ORM^{TM} are made from waste or overstock rubber products resulting in lower production cost. With the increasing of waste tire, the price superiority is more obvious, compared with the traditional H_2S adsorbents, such as activated carbon. The biggest challenge is increasing the adsorption capacity. By investigating the H_2S adsorption mechanisms, this research suggests some ways to improve the performance of TDRP^{TM} and ORM^{TM}. First of all, the research shows that higher moisture content can increase the adsorption capacity dramatically. This is the easiest way for the H_2S removal device in waste water treatment plant or other institutions. Considering some applications of biogas require low H_2S and water concentrations, such as biofuel battery, a water removal column could be installed after the TDRP^{TM} or ORM^{TM} H_2S removal column. Secondly, in the research, the particle size of TDRP^{TM} or ORM^{TM} was shown to influence the adsorption capacity.

Smaller size particles have better performance, especially for TDRP™. This indicates that the TDRP™ or ORM™ should be processed to provide a high surface area to improve adsorption capacity. Finally, the zinc or other metal concentrations in TDRP™ or ORM™ also increase the H_2S adsorption capacity. This suggests the loss of metal should be avoided during the production process.

The fundamental information TDRP™ or ORM™, characteristics and properties, can also be used for practical application. The packing and particle density are useful to calculate the porosity and packing volume during the engineering application of H_2S removal. The TGA results show the thermal stability of TDRP™ and ORM™ is reliable for temperatures less than 200 ˚C. This suggests that TDRP™ or ORM™ can be used for H_2S removal at higher temperatures, but the effect of temperature on adsorption capacity at higher temperatures requires further study. Other information, such as pH and surface area can help engineers understand TDRP™ and ORM™ well and consider the properties during the practical application of H_2S removal.

Understanding the properties and H_2S adsorption capacity of TDRP™ or ORM™ not only provides useful information for industrial H_2S removal, but also helps identify potential applications for other gaseous pollutants which have similar properties to H_2S. For example, if the gas can react with zinc or if the gas can be oxidized by functionality groups, it is possible that TDRP™ and OMR™ would be a suitable adsorbent.

5.2 Future study

Based on the challenges faced in the current research, future study on TDRP^{TM} adsorption mechanisms is suggested:

5.2.1 Modification for zinc extraction effect test

In the current research, only one zinc extraction rate was employed. To show the effect on H_2S adsorption capacity of less zinc, more TDRP^{TM} samples with different zinc extraction rates are needed. This could give a clear trend between the decrease in zinc concentration and H_2S adsorption capacity. Various extraction times are required to test this effect. Other extractant solutions would be employed, such as hydrochloric acid. The other acids would be a supplement for the zinc extraction test since HCl solution has a low oxidation potential. This could help to understand the acid solution extraction's effect on H_2S adsorption capacity of TDRP^{TM} or ORM^{TM}. By comparing the result with HNO_3 extraction results, the role of functionalities on H_2S adsorption mechanism could be determined.

5.2.2 Quantity analysis of functionalities' effect

Although the Boehm titration method failed to work for TDRP^{TM} and ORM^{TM} samples, an alternative method should be applied to determine the concentration of surface

functionalities. By quantifying the surface chemistry better, a relationship between functionalities and H_2S adsorption capacity could be established to investigate the adsorption mechanism.

5.2.3 Temperature effect and desorption research

A copper column could be made to test the effect of temperature, which would replace the PVC column in the current test device. The column would have a double-skin structure which allows water to pass through the space between the outer and inner skin. The temperature of column would be controlled by the passing water through a thermal jacket. The effect of temperature on H_2S adsorption can be determined by establishing a relationship between temperature and adsorption capacity. Besides evaluating adsorption at a higher temperature, a desorption test can be run with proper temperature control. After saturating TDRP^{TM} or ORM^{TM} with H_2S gas, nitrogen gas could be pumped in the column to test desorption behavior at different temperatures. The desorption energy, which is an important information for adsorption analysis, could be related to the reaction properties and adsorption types.

5.2.4 Looking for intermediate and final products of H_2S

As mentioned, it is hard to find intermediate and final products since the original TDRP^{TM} and ORM^{TM} contains large amounts of sulfur. However, these products are

the most direct evidences for the adsorption mechanism. To fulfill this, there are two possible methods. One method relies on removal of the original sulfur from TDRP^{TM} and ORM^{TM}. However, the influence of sulfur removal process on H_2S adsorption is unpredictable, which needs more investigation. The test may eliminate the sulfur removal effect. However, the adsorption capacity must still be evaluated. The second method exploits adsorption of additional H_2S on TDRP^{TM} or ORM^{TM}. By increasing contact time and concentration of H_2S inlet gas, a significant sulfur concentration difference between the original TDRP^{TM} or ORM^{TM} and H_2S-saturated TDRP^{TM} or ORM^{TM} is expected to appear. If either approach is successful, the next step is to characterize the sulfur formation on the surface. XPS and other surface analysis instruments could help to determinate this. If so, by calculating H_2S adsorption capacity and sulfur formation and concentration, further data would help elucidate the H_2S adsorption mechanisms of TDRP^{TM} and ORM^{TM} observed in the current research.

REFERENCES

Adhikari, B.; De, D.; Maiti, S. (2000) Reclamation and Recycling of Waste Rubber. *Progress in polymer science*, **25** (7), 909-948.

Adib, F.; Bagreev, A.; Bandosz, T. (1999) Effect of Surface Characteristics of Wood-Based Activated Carbons on Adsorption of Hydrogen Sulfide. *Journal of colloid and interface science*, **214** (2), 407-415.

Almarri, M.; Ma, X.; Song, C. (2009) Role of Surface Oxygen-Containing Functional Groups in Liquid-Phase Adsorption of Nitrogen Compounds on Carbon-Based Adsorbents. *Energy & Fuels*, 3940–3947.

Alonso-Lemus, I.; Verde, Y.; Álvarez-Contreras, L. (2009) Doped Mesoporous Materials as Pem Fuel Cell Electrocatalyst Support. ECS: p 902-930.

Bagreev, A.; Bandosz, T. (2000) Study of Hydrogen Sulfide Adsorption on Activated Carbons Using Inverse Gas Chromatography at Infinite Dilution. *J. Phys. Chem. B*, **104** (37), 8841-8847.

Bagreev, A.; Bandosz, T. (2001) H_2s Adsorption/Oxidation on Unmodified Activated Carbons: Importance of Prehumidification. *Carbon*, **39** (15), 2303-2311.

Bandosz, T. (1999) Effect of Pore Structure and Surface Chemistry of Virgin Activated Carbons on Removal of Hydrogen Sulfide. *Carbon*, **37** (3), 483-491.

Barton, B. (1950) Use of Oxidizing Agents in Rubber Vulcanization-Zinc Oxide-Free Process. *Industrial & Engineering Chemistry*, **42** (4), 671-674.

Bignozzi, M.; Sandrolini, F. (2006) Tyre Rubber Waste Recycling in Self-Compacting Concrete. *Cement and Concrete Research*, **36** (4), 735-739.

Biniak, S.; Szyma ski, G.; Siedlewski, J.; wia tkowski, A. (1997) The Characterization of Activated Carbons with Oxygen and Nitrogen Surface Groups. *Carbon*, **35** (12), 1799-1810.

Boehm, H. (1966) Chemical Identification of Surface Groups. *Advances in catalysis*, **16** 179-274.

Boudou, J.; Chehimi, M.; Broniek, E.; Siemieniewska, T.; Bimer, J. (2003) Adsorption of H_2s or So_2 on an Activated Carbon Cloth Modified by Ammonia Treatment. *Carbon*, **41** (10), 1999-2007.

Bouzaza, A.; Laplanche, A.; Marsteau, S. (2004) Adsorption–Oxidation of Hydrogen Sulfide on Activated Carbon Fibers: Effect of the Composition and the Relative Humidity of the Gas Phase. *Chemosphere*, **54** (4), 481-488.

Brandt, R.; Hughes, M.; Bourget, L.; Truszkowska, K.; Greenler, R. (1993) The Interpretation of Co Adsorbed on Pt/Sio2 of Two Different Particle-Size Distributions. *Surface Science*, **286** (1-2), 15-25.

Chatterjee, G.; Houde, A.; Stern, S. (1997) Poly (Ether Urethane) and Poly (Ether Urethane Urea) Membranes with High H_2s/Ch_4 Selectivity. *Journal of Membrane Science*, **135** (1), 99-106.

Colom, X.; Carrillo, F.; Canavate, J. (2007) Composites Reinforced with Reused Tyres: Surface Oxidant Treatment to Improve the Interfacial Compatibility. *Composites Part A*, **38** (1), 44-50.

Dave, A. (2009) Occurrence and Effects of Tire Wear Particles in the Environment-a Critical Review and an Initial Risk Assessment. *Environmental Pollution*, **157** (1-11).

Ellis, T. G.; Park, J.; Oh, J. (2008) *A Novel and Cost-Effective H2s Absorption Technology Using Tire Derived Rubber Particles*.

Entezari, M.; Ghows, N.; Chamsaz, M. (2005) Combination of Ultrasound and Discarded Tire Rubber: Removal of Cr (Iii) from Aqueous Solution. *Journal of Physical Chemistry A*, **109** (20), 4638-4642.

Garcia, C.; Lercher, J. (1992) Adsorption of Hydrogen Sulfide on Zsm 5 Zeolites. *The Journal of Physical Chemistry*, **96** (5), 2230-2235.

Gualtieri, M.; Andrioletti, M.; Vismara, C.; Milani, M.; Camatini, M. (2005) Toxicity of Tire Debris Leachates. *Environment international*, **31** (5), 723-730.

Haimour, N.; El-Bishtawi, R.; Ail-Wahbi, A. (2005) Equilibrium Adsorption of Hydrogen Sulfide onto Cuo and Zno. *Desalination*, **181** (1-3), 145-152.

Hamadi, N.; Chen, X.; Farid, M.; Lu, M. (2001) Adsorption Kinetics for the Removal of Chromium (Vi) from Aqueous Solution by Adsorbents Derived from Used Tyres and Sawdust. *Chemical Engineering Journal*, **84** (2), 95-105.

Hao, J.; Rice, P.; Stern, S. (2002) Upgrading Low-Quality Natural Gas with H2s-and Co2-Selective Polymer Membranes Part I. Process Design and Economics of Membrane Stages without Recycle Streams. *Journal of Membrane Science*, **209** (1), 177-206.

Heideman, G.; Datta, R.; Noordermeer, J.; Baarle, B. (2005) Influence of Zinc Oxide During Different Stages of Sulfur Vulcanization. Elucidated by Model Compound Studies. *Journal of Applied Polymer Science*, **95** (6), 1388-1404.

Hernandez-Olivares, F.; Barluenga, G.; Bollati, M.; Witoszek, B. (2002) Static and Dynamic Behaviour of Recycled Tyre Rubber-Filled Concrete. *Cement and Concrete Research*, **32** (10), 1587-1596.

Kapdi, S.; Vijay, V.; Rajesh, S.; Prasad, R. (2005) Biogas Scrubbing, Compression and Storage: Perspective and Prospectus in Indian Context. *Renewable energy*, **30** (8), 1195-1202.

Kim, J.; Park, J.; Edil, T. (1997) Sorption of Organic Compounds in the Aqueous Phase onto Tire Rubber. *Journal of Environmental Engineering*, **123** (9), 827-835.

Krishnankutty, N.; Vannice, M. (1995) Effect of Pretreatment on Surface Area, Porosity, and Adsorption Properties of a Carbon Black. *Chemistry of materials*, **7** (4), 754-763.

Leblanc, J. (2002) Rubber–Filler Interactions and Rheological Properties in Filled Compounds. *Progress in polymer science*, **27** (4), 627-687.

Lehmann, C.; Rostam-Abadi, M.; Rood, M.; Sun, J. (1998) Reprocessing and Reuse of Waste Tire Rubber to Solve Air-Quality Related Problems. *Energy Fuels*, **12** (6), 1095-1099.

Leung, D.; Yin, X.; Zhao, Z.; Xu, B.; Chen, Y. (2002) Pyrolysis of Tire Powder: Influence of Operation Variables on the Composition and Yields of Gaseous Product. *Fuel Processing Technology*, **79** (2), 141-155.

Li, G.; Stubblefield, M.; Garrick, G.; Eggers, J.; Abadie, C.; Huang, B. (2004) Development of Waste Tire Modified Concrete. *Cement and Concrete Research*, **34** (12), 2283-2289.

Lin, C.; Huang, C.; Shern, C. (2008) Recycling Waste Tire Powder for the Recovery of Oil Spills. *Resources, Conservation & Recycling*, **52** (10), 1162-1166.

Lisi, R.; Park, J.; Stier, J. (2004) Mitigating Nutrient Leaching with a Sub-Surface Drainage Layer of Granulated Tires. *Waste Management*, **24** (8), 831-839.

Loadman, M. J. R. (1998) Analysis of Rubber and Rubber-Like Polymers, kluwer academic publishers

Manchon-Vizuete, E.; Macias-Garcia, A.; Nadal Gisbert, A.; Fernandez-Gonzalez, C.; Gomez-Serrano, V. (2005) Adsorption of Mercury by Carbonaceous Adsorbents Prepared from Rubber of Tyre Wastes. *Journal of Hazardous Materials*, **119** (1-3), 231-238.

Mbah, J.; Krakow, B.; Stefanakos, E.; Wolan, J. (2008) Electrolytic Splitting of H_2s Using Cshso Membrane. *Journal of The Electrochemical Society*, **155** 166-170.

Meng, X.; Hua, Z.; Dermatas, D.; Wang, W.; Kuo, H. (1998) Immobilization of Mercury (Ii) in Contaminated Soil with Used Tire Rubber. *Journal of Hazardous Materials*, **57** (1-3), 231-241.

Miguel, G.; Fowler, G.; DallOrso, M.; Sollars, C. (2002) Porosity and Surface Characteristics of Activated Carbons Produced from Waste Tyre Rubber. *Journal of Chemical Technology &# 38; Biotechnology*, **77** (1), 1-8.

Novochinskii, I.; Song, C.; Ma, X.; Liu, X.; Shore, L.; Lampert, J.; Farrauto, R. (2004) Low-Temperature H_2s Removal from Steam-Containing Gas Mixtures with Zno for Fuel Cell Application. 1. Zno Particles and Extrudates. *Energy and Fuels*, **18** (2), 576-583.

Pantea, D.; Darmstadt, H.; Kaliaguine, S.; Roy, C. (2003) Heat-Treatment of Carbon Blacks Obtained by Pyrolysis of Used Tires. Effect on the Surface Chemistry,

Porosity and Electrical Conductivity. *Journal of Analytical and Applied Pyrolysis*, **67** (1), 55-76.

Papirer, E.; Lacroix, R.; Donnet, J. (1996) Chemical Modifications and Surface Properties of Carbon Blacks. *Carbon*, **34** (12), 1521-1529.

Park, D.; Lee, D.; Joung, J.; Park, J. (2005) Comparison of Different Bioreactor Systems for Indirect H2s Removal Using Iron-Oxidizing Bacteria. *Process Biochemistry*, **40** (3-4), 1461-1467.

Park, J. (2004) Effectiveness of Scrap Tire Chips as Sorptive Drainage Material. *Journal of Environmental Engineering*, **130** 824.

Patnaik, P. (2002) Handbook of Inorganic Chemicals, McGraw-Hill Professional.

Pehlken, A.; Müller, D. (2009) Using Information of the Separation Process of Recycling Scrap Tires for Process Modelling. *Resources, Conservation & Recycling*, **54** 140-148.

Pierce, C.; Blackwell, M. (2003) Potential of Scrap Tire Rubber as Lightweight Aggregate in Flowable Fill. *Waste Management*, **23** (3), 197-208.

Potivichayanon, S.; Pokethitiyook, P.; Kruatrachue, M. (2006) Hydrogen Sulfide Removal by a Novel Fixed-Film Bioscrubber System. *Process Biochemistry*, **41** (3), 708-715.

Purakayastha, P.; Pal, A.; Bandyopadhyay, M. (2002) Adsorption of Anionic Surfactant by a Low-Cost Adsorbent. *Journal of environmental science and health. Part A, Toxic/hazardous substances & environmental engineering*, **37** (5), 925-938.

Purakayastha, P.; Pal, A.; Bandyopadhyay, M. (2005) Sorption Kinetics of Anionic Surfactant on to Waste Tire Rubber Granules. *Separation and Purification Technology*, **46** (3), 129-135.

Putman, B.; Amirkhanian, S. (2004) Utilization of Waste Fibers in Stone Matrix Asphalt Mixtures. *Resources, Conservation & Recycling*, **42** (3), 265-274.

Ranade, D.; Dighe, A.; Bhirangi, S.; Panhalkar, V.; Yeole, T. (1999) Evaluation of the Use of Sodium Molybdate to Inhibit Sulphate Reduction During Anaerobic Digestion of Distillery Waste. *Bioresource technology*, **68** (3), 287-291.

Rodgers, B. (2004) Rubber Compounding –Chemistry and Applications, Marcel Dekker, Inc.

Segre, N.; Monteiro, P.; Sposito, G. (2002) Surface Characterization of Recycled Tire Rubber to Be Used in Cement Paste Matrix. *Journal of colloid and interface science*, **248** (2), 521-523.

Segre, N.; Joekes, I.; Galves, A.; Rodrigues, J. (2004) Rubber-Mortar Composites: Effect of Composition on Properties. *Journal of Materials Science*, **39** (10), 3319-3327.

Seredych, M.; Strydom, C.; Bandosz, T. (2008) Effect of Fly Ash Addition on the Removal of Hydrogen Sulfide from Biogas and Air on Sewage Sludge-Based Composite Adsorbents. *Waste Management*, **28** (10), 1983-1992.

Shah, J.; Jan, M.; Mabood, F.; Shahid, M. (2006) Conversion of Waste Tyres into Carbon Black and Their Utilization as Adsorbent. *Journal of the Chinese Chemical Society*, **53** (5), 1085-1089.

Siddique, R.; Naik, T. (2004) Properties of Concrete Containing Scrap-Tire Rubber–an Overview. *Waste Management*, **24** (6), 563-569.

Smolders, E.; Degryse, F. (2002) Fate and Effect of Zinc from Tire Debris in Soil. *Environ. Sci. Technol*, **36** (17), 3706-3710.

Soreanu, G.; Béland, M.; Falletta, P.; Edmonson, K.; Seto, P. (2008) Laboratory Pilot Scale Study for H_2s Removal from Biogas in an Anoxic Biotrickling Filter. *Water Science and Technology*, **57** (2), 201-208.

Studebaker, M.; Huffman, E.; Wolfe, A.; Nabors, L. (1956) Oxygen-Containing Groups on the Surface of Carbon Black. *Industrial & Engineering Chemistry*, **48** (1), 162-166.

Tien, C. (1994) Adsorption Calculations and Modeling, Butterworth-Heinemann Boston.

Truong, L.; Abatzoglou, N. (2005) A H_2s Reactive Adsorption Process for the Purification of Biogas Prior to Its Use as a Bioenergy Vector. *Biomass and Bioenergy*, **29** (2), 142-151.

Tsai, J.; Jeng, F.; Chiang, H. (2001) Removal of H_2s from Exhaust Gas by Use of Alkaline Activated Carbon. *Adsorption*, **7** (4), 357-366.

Ucar, S.; Karagoz, S.; Ozkan, A.; Yanik, J. (2005) Evaluation of Two Different Scrap Tires as Hydrocarbon Source by Pyrolysis. *Fuel*, **84** (14-15), 1884-1892.

Van der Zee, F.; Villaverde, S.; Garcia, P.; Fdz.-Polanco, F. (2007) Sulfide Removal by Moderate Oxygenation of Anaerobic Sludge Environments. *Bioresource technology*, **98** (3), 518-524.

Verleye, G. A. L.; Roeges, N. P. G.; Moor, M. O. D. (2001) Easy Identification of Plastics and Rubbers RAPRA technology LTD.

Williams, P.; Besler, S. (1995) Pyrolysis-Thermogravimetric Analysis of Tyres and Tyre Components. *Fuel*, **74** (9), 1277-1283.

Xiao, F.; Amirkhanian, S.; Shen, J.; Putman, B. (2009) Influences of Crumb Rubber Size and Type on Reclaimed Asphalt Pavement (Rap) Mixtures. *Construction and Building Materials*, **23** (2), 1028-1034.

Xiao, Y.; Wang, S.; Wu, D.; Yuan, Q. (2008) Experimental and Simulation Study of Hydrogen Sulfide Adsorption on Impregnated Activated Carbon under Anaerobic Conditions. *Journal of Hazardous Materials*, **153** (3), 1193-1200.

Yang, R. T. (2003) Adsorbents ---Fundamentals and Applications john wiley & sons, INC.

Yuan, W.; Bandosz, T. (2007) Removal of Hydrogen Sulfide from Biogas on Sludge-Derived Adsorbents. *Fuel*, **86** (17-18), 2736-2746.

ATSDR (2008) Minimal Risk Levels (MRLs) for Hazardous Substances. *Agency for Toxic Substances and Disease Registry. URL: http://www.atsdr.cdc.gov/mrls/*

OEHHA (2007) Evaluation of Health Effects of Recycled Waste Tires in Playground and Track Products. *Calrecycle. URL: http://www.calrecycle.ca.gov /publications/Tires/62206013.pdf*

Jenö Kovács (2007) What is Anaerobic Digestion Process for Producing Biogas? *URL: www.handbook.ifrf.net/handbook/dl.html/index.pdf?id=81&type=pdf "Basic information on biogas"*

EPA (2003) Toxicological Review of Hydrogen Sulfide. *URL: www.epa.gov/iris*

EPA (2008). Wastes - Resource Conservation - Common Wastes & Materials - Scrap Tires. *URL: http://www.epa.gov/osw/conserve/materials/tires/basic.htm*

Wikipedia (2010). Langmuir equation. *wikipedia.org. URL: http://en.wikipedia.org/ wiki/Langmuir_isotherm*

APPENDIX

Table 1a. physical properties of Hydrogen sulfide.

	Hydrogen Sulfide (H2S)
Molecular Weight (g/mol)	34.08
Melting Point (Tm, K)	187.65
Boiling Point (Tb, K)	212.45
Critical Point (Tc, K)	---
Density (g/cm3)	1.54

Table 2a. Carbon black group by surface area (Rodgers, 2004).

Group No.	Ave. N_2 surface area (m^2/g)
0	>150
1	121-150
2	100-120
3	70-99
4	50-69
5	40-49
6	22-39
7	21-32
8	11-20
9	0-10

Table 3a. Packing density of TDRP™ and ORM™.

Beaker weight (g)	61.64
After packing with ORM™ (g)	91.38
After packing with TDRP™ (g)	106.25
Density of ORM™ (Kg/m^3)	0.21
Density of TDRP™ (Kg/m^3)	0.31

Table 4a. Particle density of TDRP™ and ORM™.

Item	ORM™ test 1	ORM™ test 2	TDRP™ test 1	TDRP™ test 2	TDRP™ test 3
Mass of dried TDRP™/ORM™ (g)	2	2	3	3	3
V1 (mL)	28.0	27.8	19.7	20.5	18.1
V2 (mL)	30.0	30.0	32.0	33.1	31.2
Specific Density (g/mL)	1	0.9	1.3	1.2	1.4
Average (g/mL)		1.0			1.3

Table 5a. Moisture content of TDRP™ and ORM™.

Item	ORM™		TDRP™			
Beaker weight (g)	51.1751	26.7281	23.6801	51.3281	23.5514	25.0209
Beaker with TDRP™/ORM™ (g)	60.0833	31.0373	28.3936	62.2917	28.7419	30.1594
Beaker weight after heating (g)	60.0016	30.9707	28.3243	62.2600	28.8419	30.1264
Initial TDRP™/ORM™ mass (g)	8.9082	4.3092	4.7135	10.9636	5.1905	5.1385
Dried TDRP™/ORM™ mass (g)	8.8279	4.2426	4.6442	10.9365	5.2905	5.1055
Moisture content	0.9%	1.55%	1.47%	0.25%	0.79%	0.64%
Average moisture content			1.31%			0.56%

Table 6a. Surface pH of TDRP™ and ORM™.

pH	Blank	ORM™	TDRP™
Test 1	6.02	10.7	8.56
Test 2		11.05	8.84
Test 3		11.05	8.70
Average		10.93	8.70

Table 7a. Surface oxidation function group of TDRP™ or ORM™.

	$NaHCO_3$		Na_2CO_3		NaOH	
TDRP™/ORM™ (0.25g)	A	B	A	B	A	B
Sample volume (mL)	10.0	10.0	10.0	10.0	10.0	10.0
0.05M HCl (mL)	39.0	20.0	30.0	30.0	20.0	20.0
0.05M NaOH (mL) for titration	33.5	16.8	17.3	17.7	10.0	9.8
Chemicals consumed by TDRP™/ORM™ (mL)	4.5	6.8	7.3	7.7	0	0.2
Oxidation function group types	carboxylic groups		carboxylic and lactonic groups		Carboxylic, lactonic, and phenolic groups	
Oxidation function group conc. (mol/g)	0.0018	0.0027	0.0029	0.0031	0	0.8×10^{-7}

Table 8a. Surface Functionalities of TDRP™ and ORM™.

	NaOH 1		NaOH 2	
TDRP™/ ORM™ (0.5 g)	A	B	A	B
Sample volume (mL)	20.00	20.00	20.00	20.00
0.05M HCl (mL)	30.00	30.00	30.00	30.00
0.05M NaOH (mL) for titration	11.11	12.89	10.85	11.38
Chemicals consumed by TDRP™/ORM™ (mL)	1.11	2.89	0.85	1.38
Oxidation function group types	Carboxylic, lactonic, and phenolic groups			
Oxidation function group conc. (mol/g)	1.11×10^{-4}	2.89×10^{-4}	0.85×10^{-4}	1.38×10^{-4}

Table 9a. TDRP™ and ORM™ adsorption capacity.

	Adsorption capacity (mg/g)		Time to 100ppm (min)	
	Test 1	Test 2	Test 1	Test 2
ORM™	0.7265	0.8120	163.6	180.4
TDRP™	0.3547	0.4057	138.4	182.6

Table 10a. Adsorption capacity of TDRP™ with different $ZnCl_2$.

	Zn concentration (g/g)	Adsorption capacity (mg/g)	Time to 100ppm (min)
TDRP™	0.01422	0.4941	138.4
0.21g $ZnCl_2$ (0.099g Zinc) added	0.01917	0.6390	143.4
0.43g $ZnCl_2$ (0.203g Zinc) added	0.02438	0.9536	203.6
0.65g $ZnCl_2$ (0.309g Zinc) added	0.02969	1.1749	227.1

Table 11a. adsorption capacity of zinc-extraction TDRP™.

Items	H_2S adsorption capacity (mg/g)		
	Test 1	Test 2	Average
TDRP™ without HNO_3 extraction	0.086	0.159	0.123
TDRP™ with HNO_3 extraction	0.103	0.159	0.131
TDRP™ without NaOH extraction	0.105	0.124	0.115
TDRP™ with NaOH extraction	0.065	0.055	0.060

Table 12a. Adsorption capacity of different radius TDRP™ and ORM™ samples.

ORM™				
size	<0.6 mm	0.6~1 mm	>1m m	no size classification
Adsorption capacity mg/g TEST 1	0.250	0.225	0.191	
TEST 2	0.350	0.242	0.239	
Average	0.300	0.234	0.215	
Ration by Weight %	46.0%	21.0%	33.0 %	
Average modified by weight ration			0.258	0.215
TDRP™				
size	<0.6 mm	0.6~1 mm	>1m m	no size classification
Adsorption capacity mg/g TEST 1	0.164	0.109	0.004	
TEST 2	0.134	0.138	0.094	
TEST 3	0.126	0.097	0.036	
Average	0.142	0.115	0.045	
Ration by Weight %	55.0%	34.0%	11.0 %	
Average modified by weight ration			0.122	0.119

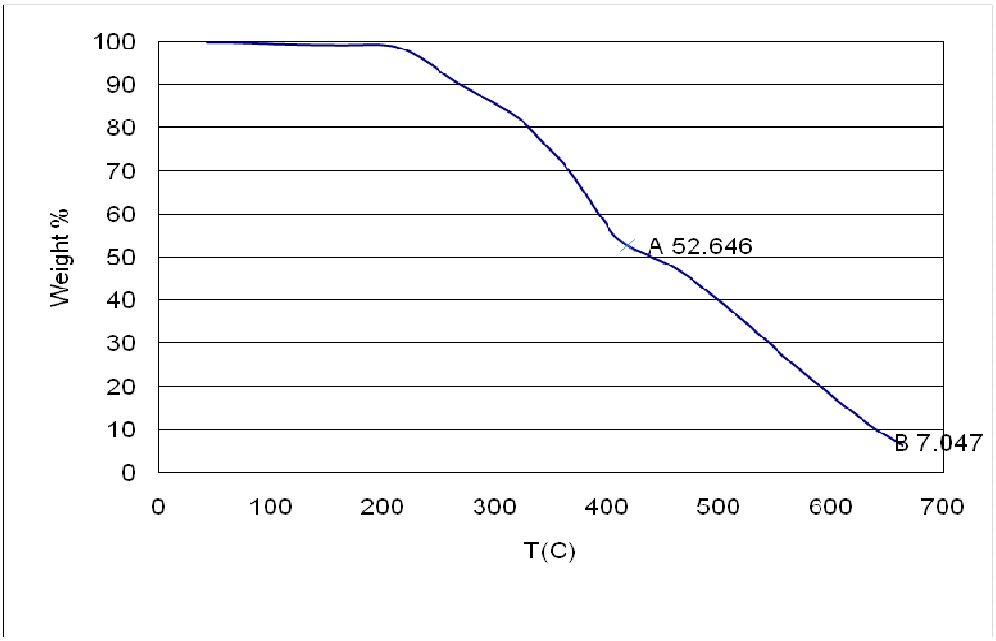

Figure 1a. TGA analysis of ORM™.

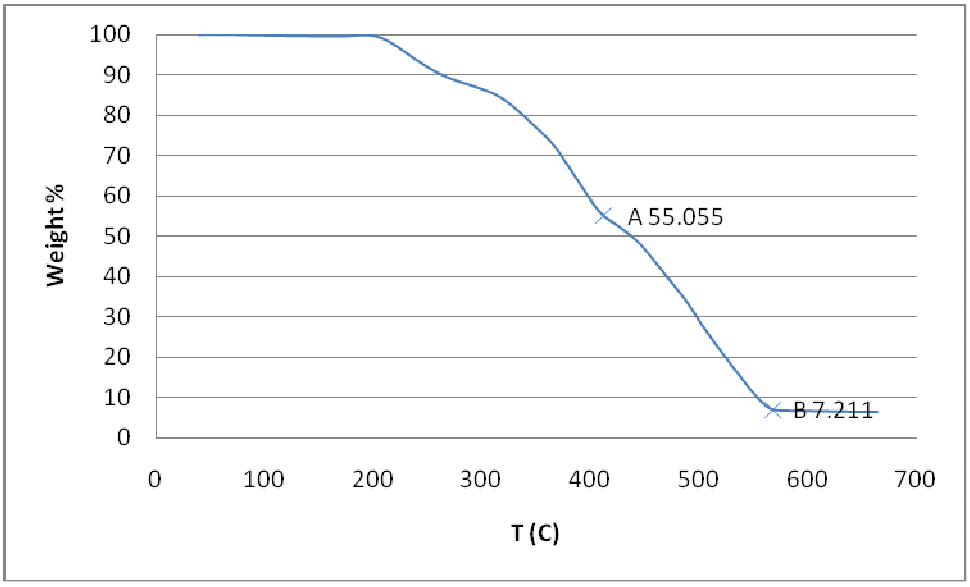

Figure 2a. TGA result of TDRP™.

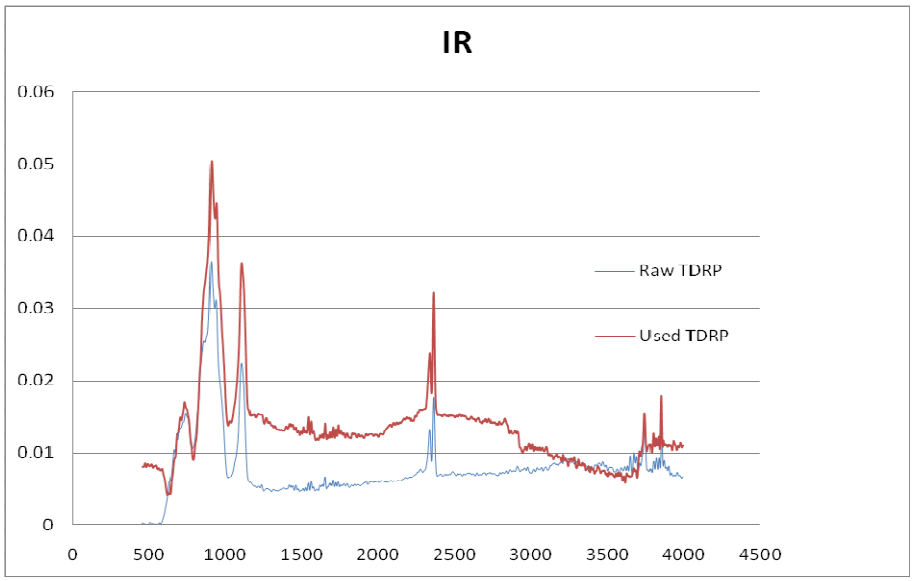

Figure 3a. Infrared result of TDRP^{TM}.

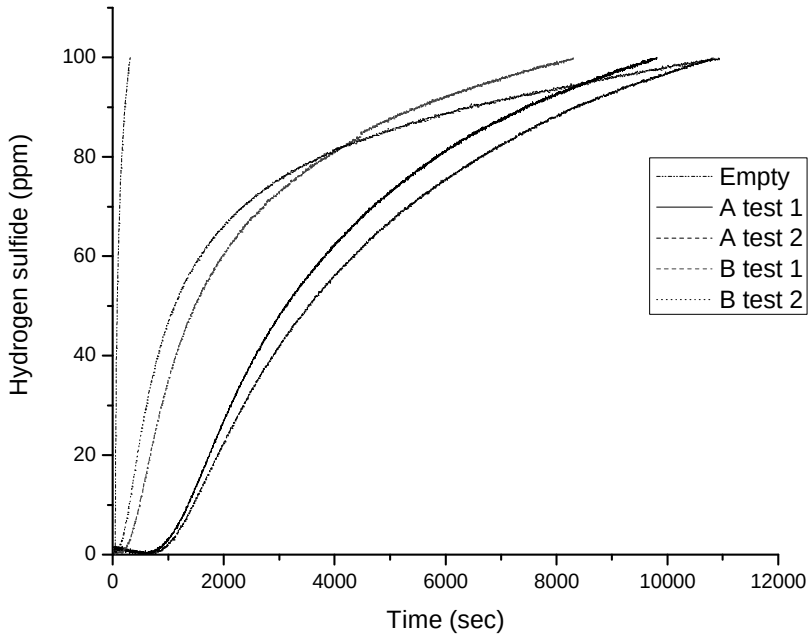

Figure 4a. H2S breakthrough curves of ORM^{TM} (A) and TDRP^{TM} (B).

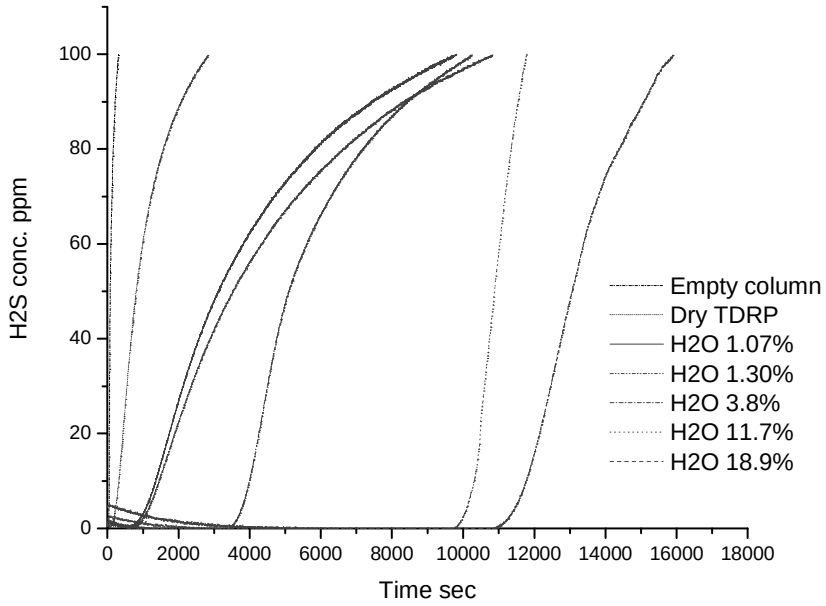

Figure 5a. H_2S breakthrough curve of ORM^{TM} with different moisture content.

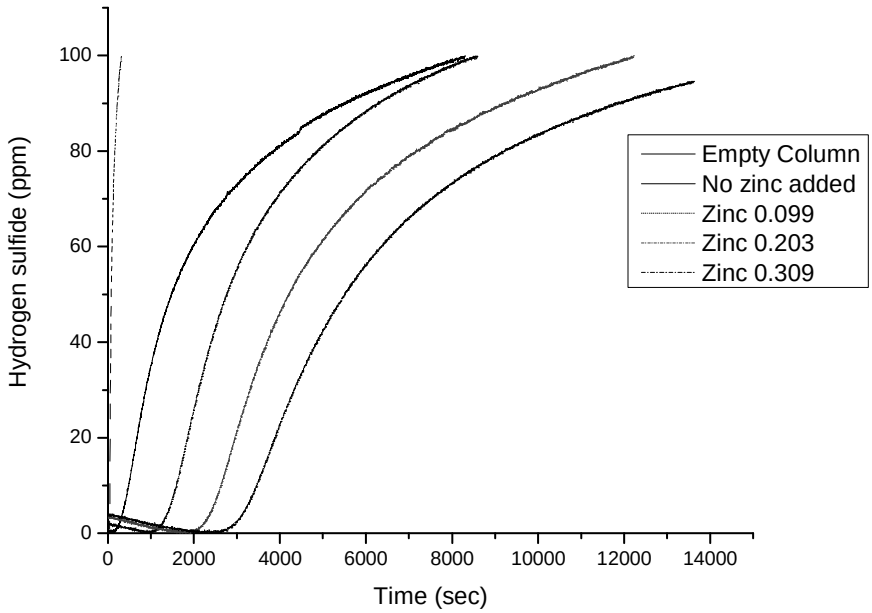

Figure 6a. H_2S breakthrough curve of TDPR with different $ZnCl_2$.

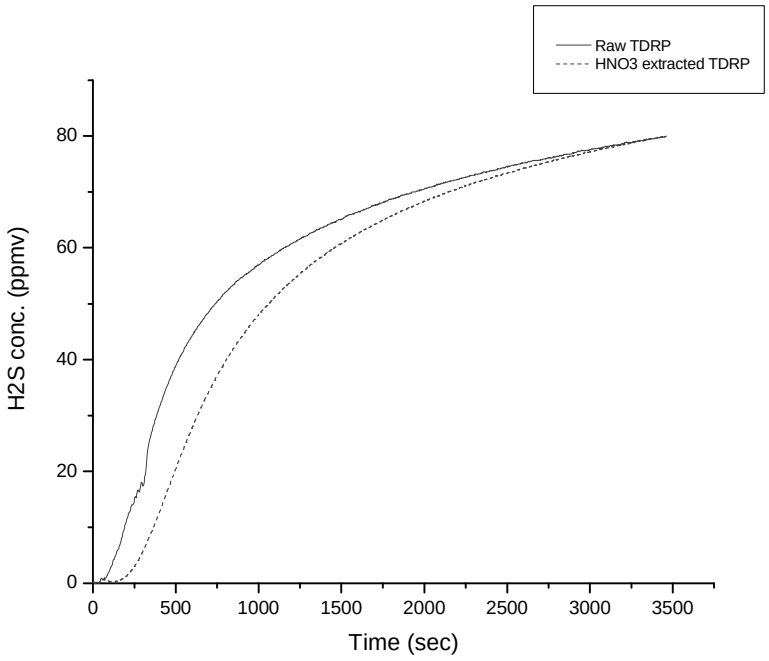

a

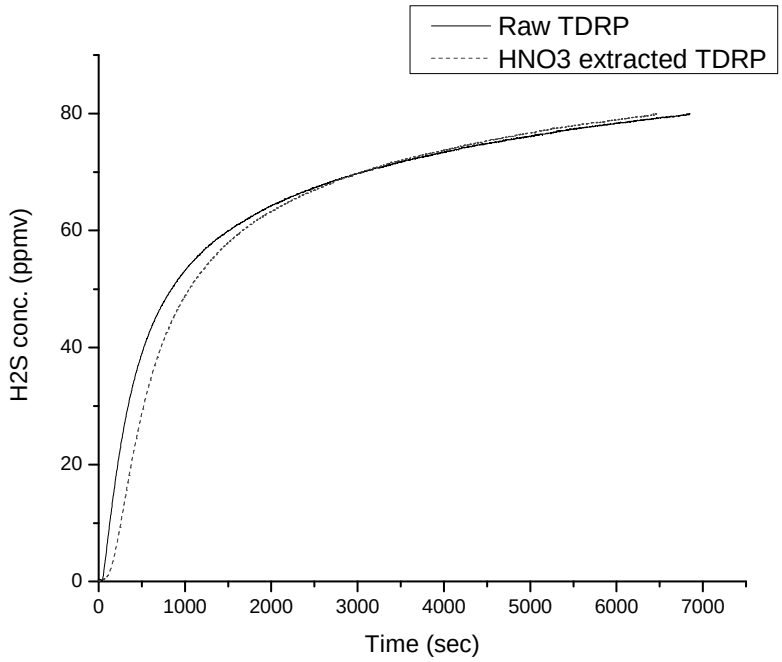

b

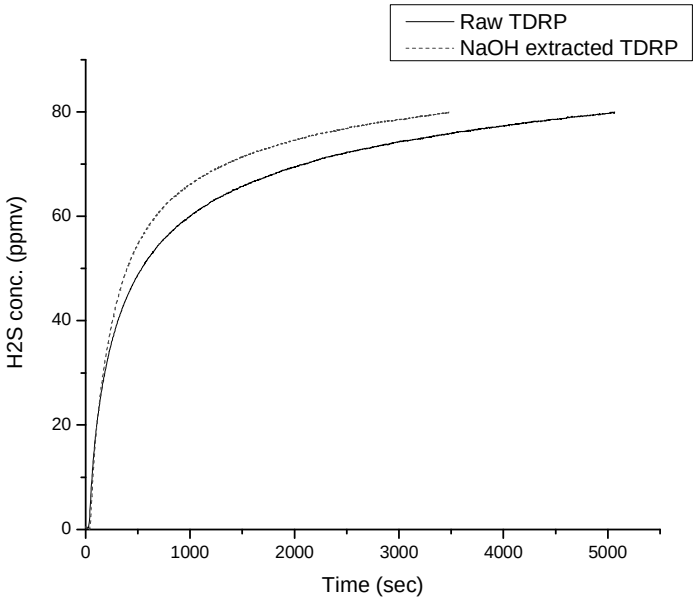

c

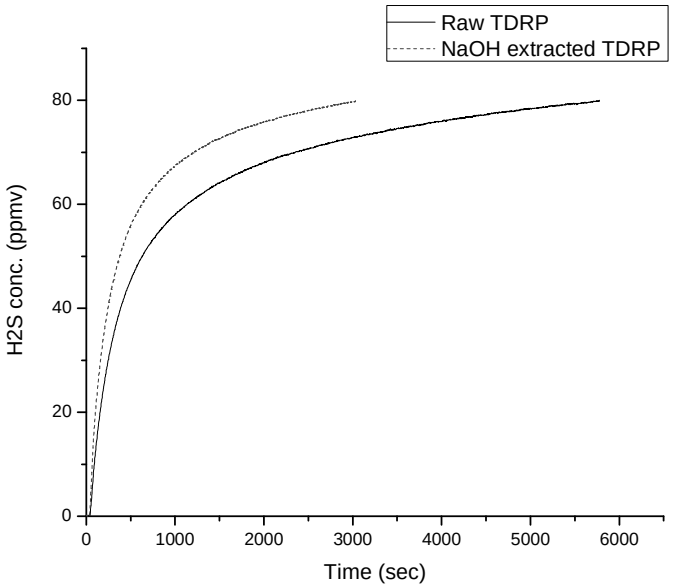

d

Figure 7a. Breakthrough curve of zinc-extraction TDRP^{TM} samples. a. HNO3-extracted TDRP^{TM} test 1; b. HNO3-extracted TDRP^{TM} test 2; c. NaOH-extracted TDRP^{TM} test 1; d. NaOH-extracted TDRP^{TM} test 2

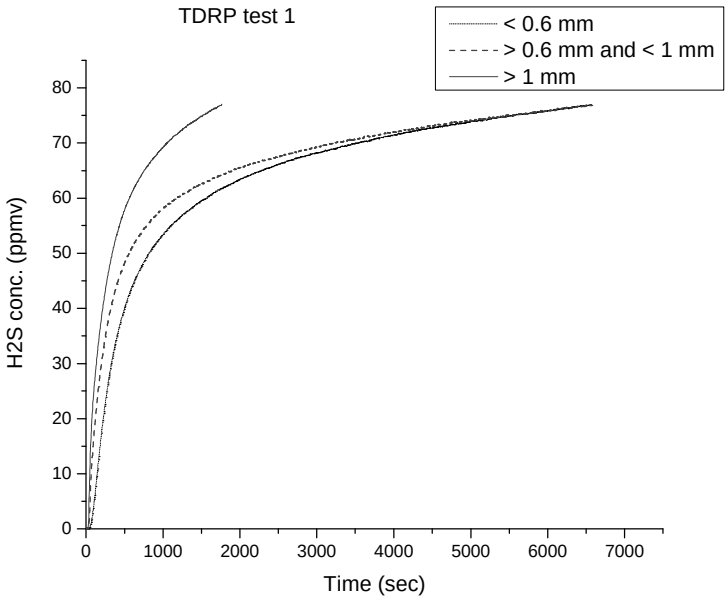

a

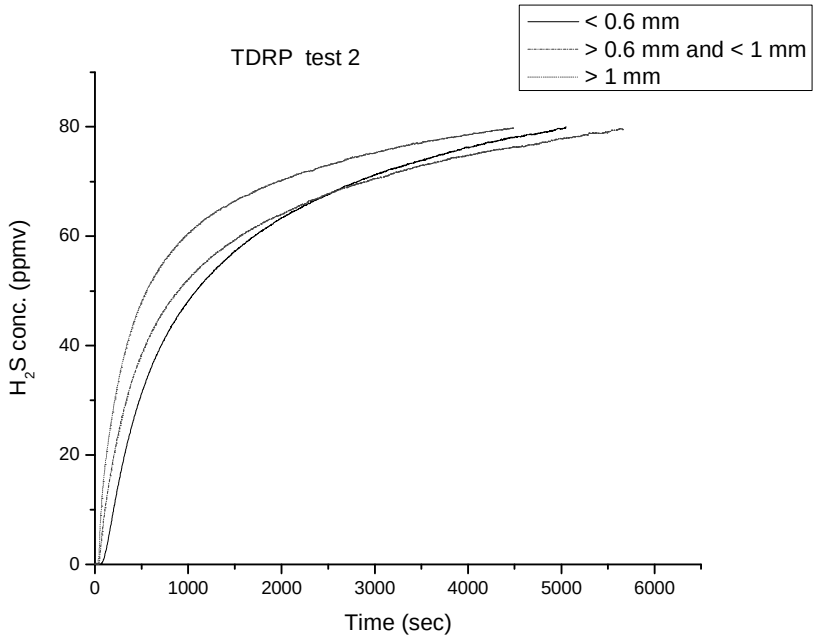

b

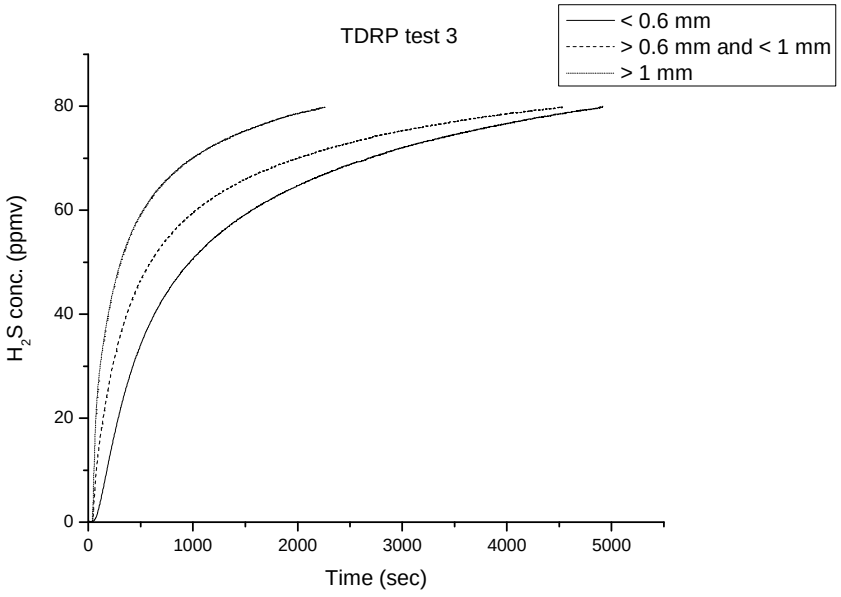

c

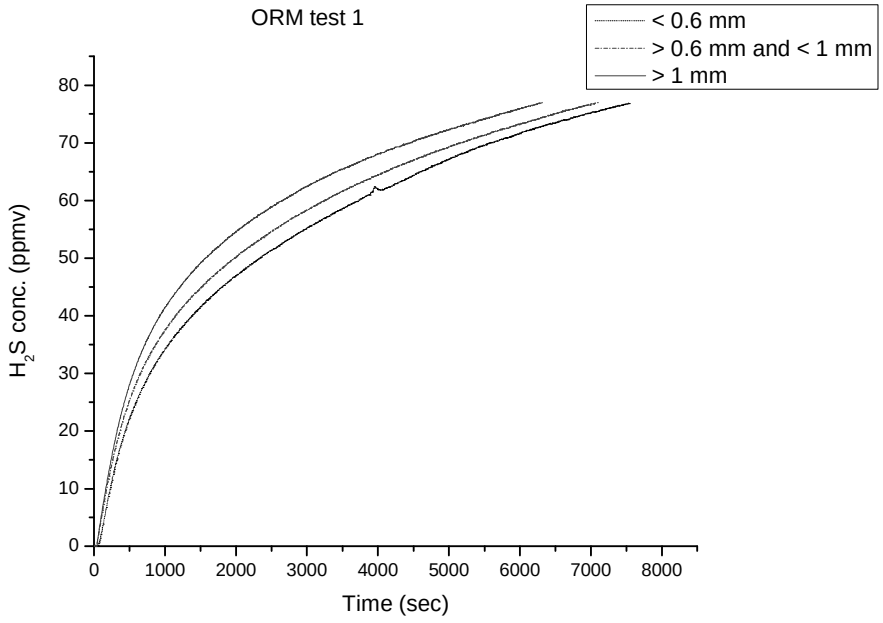

d

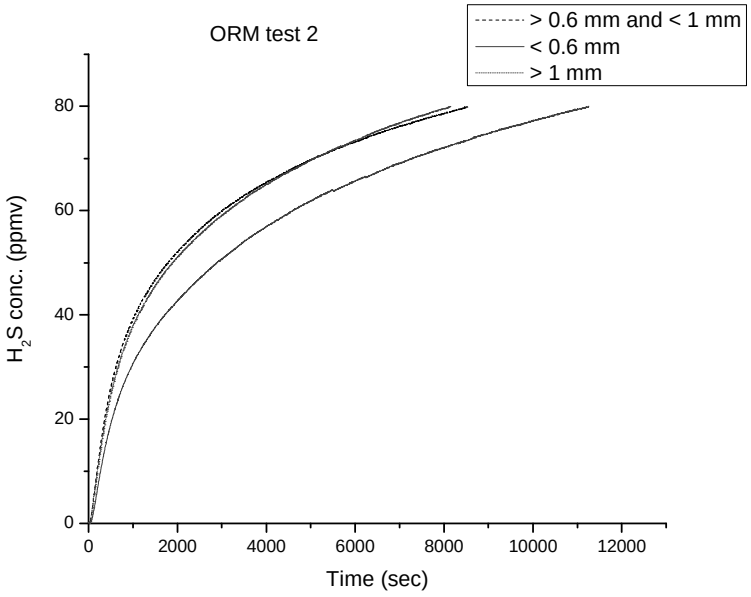

e

Figure 8a. Breakthrough curve of different size TDRP^{TM} samples. a. TDRP^{TM} test 1; b. TDRP^{TM} test 2; c. TDRP^{TM} test 3; d ORM^{TM} test 1; e ORM^{TM} test 2

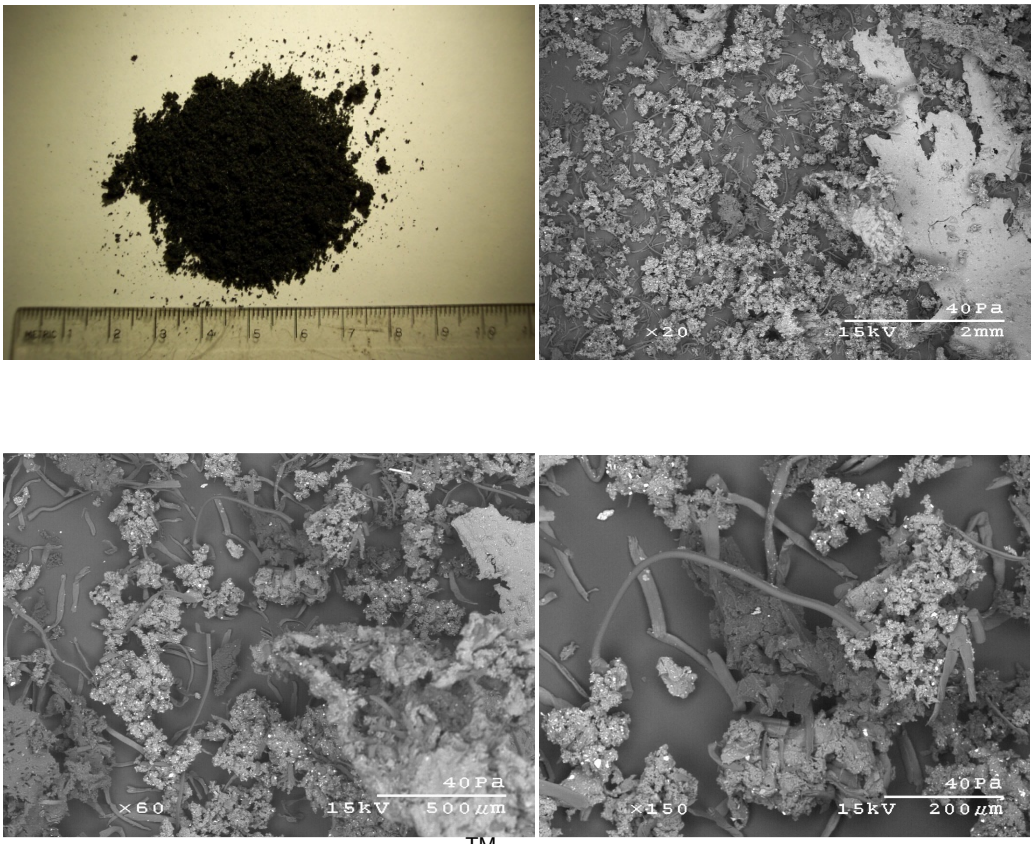

Figure 9a. SEM pictures of TDRP^{TM}.

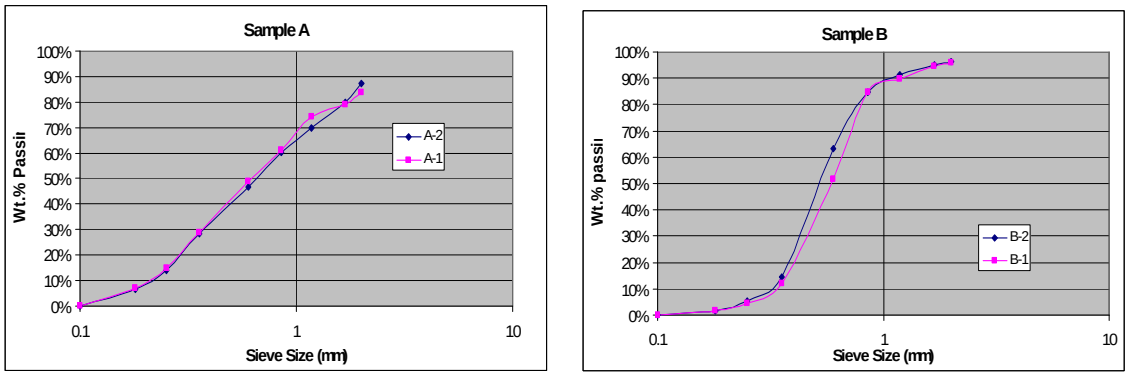

Figure 10a. size distribution of ORM^{TM} (sample A)and TDRP^{TM} (sample B) (Ellis et al., 2008).

ACKNOWLEDGEMENTS

I owe my gratitude and respect to a number of people helping me complete during my M.S. study. I am indebted to my major professor, Dr. Tim Ellis who has been my guide through my two years study. Thanks to Dr. Eric Evans, who helped me build up the experiment instruments and give me valuable advises on my research. Special thanks are extended to Andrea Siefers and Dr. Jaeyoung Park, who both gave me suggestion on my research. Thanks to Warren Straszheim and James Anderegg, who tested the samples for my research. I also want to thank to Kathy Petersen for the great help of doing university bureaucracy. Thanks to Samuel Cotter for reviewing my thesis.

Above all, thanks to my parents, Xinchuang Wang and Yuanjun Gao, for the constant encouragement. Finally thanks to the China Scholarship Council, who provided me the opportunity to study abroad.